R-02-34

Single-well injection-withdrawal tests (SWIW)

Literature review and scoping calculations for homogeneous crystalline bedrock conditions

Rune Nordqvist, Erik Gustafsson
Geosigma AB

August 2002

Svensk Kärnbränslehantering AB
Swedish Nuclear Fuel
and Waste Management Co
Box 5864
SE-102 40 Stockholm Sweden
Tel 08-459 84 00
+46 8 459 84 00
Fax 08-661 57 19
+46 8 661 57 19

ISSN 1402-3091
SKB Rapport R-02-34

Single-well injection-withdrawal tests (SWIW)

Literature review and scoping calculations for homogeneous crystalline bedrock conditions

Rune Nordqvist, Erik Gustafsson
Geosigma AB

August 2002

Abstract

This report describes a literature review and scoping calculations carried out in order to test the feasibility of using SWIW (Single Well Injection Withdrawal) tracer experiments for expected hydraulic conditions in Swedish bedrock. The motivation for using SWIW tests in the site investigation programme is that extensive cross-hole tracer tests may not be possible and that such SWIW tests are more or less the only available single-hole tracer test method. The scoping calculations are aimed at establishing conditions under which SWIW tests should be feasible, by studying experimental attributes such as expected bedrock properties (transmissivity, porosity, etc), ambient hydraulic gradients, duration of various experimental phases, hydraulic injection pressure and parameter identification possibilities. Particular emphasis has been placed on the use of the dilution probe as an experimental device for SWIW, although the scoping results also should be considered applicable to any experimental equipment approach. The results from the scoping calculations indicate that SWIW tests using the dilution probe are feasible under the required experimental and site requirements for the forthcoming site investigations programme. The characteristic flow reversibility feature inherent in SWIW tests causes some differences compared with cross-hole tracer tests. Advective parameters (i.e. mobile porosity, dispersivity) are generally more difficult to identify/estimate and the same may also be said about equilibrium sorption. Time-dependent processes, on the other hand, generally benefit from the flow reversibility, in principle even in the presence of heterogeneity. However, it may not always be possible to identify time-dependent processes, such as matrix diffusion, for expected conditions in Swedish bedrock. Experimental aims may be allowed to vary depending on the specific conditions (transmissivity, hydraulic gradient, etc.) in the tested borehole section.

Table of contents

1 Introduction

Tracer experiments have been used extensively for transport investigations in fractured rocks /see, for example Andersson, 1995/. Such experiments may roughly be divided into two major types; multi-well or single well tracer experiments. Multi-well tracer tests are appealing because they reveal transport characteristics along a flowpath between two points. On the other hand, these types of tracer tests also require a verified, by prior investigations, hydraulic connection between two points in order to be able to perform a successful experiment with high tracer recovery. Such prior investigations may be relatively extensive, including different types of hydraulic tests and a number of drilled boreholes.

Single-well tests have the advantage of being a feasible method with much less prior investigations and require only one borehole. On the other hand, the injected tracer in this type of test experiences only a limited volume of the rock most adjacent to the tested borehole section. Multi-well tests may give different types of information more relevant to flowpaths over longer distances. For interpretation of transport processes, both types of test have different advantages. For example, single-well tests provide flow reversibility, which may be argued to be an advantage for the identification and quantification of time-dependent processes.

Ideally, both types of tests would be carried out, as they give different information and may be expected to complement each other. However, in the site investigation programme, it may not always be possible to perform multi-well tests because of investigation constraints. Thus, a feasible single-well method would then be very important. This report describes a single-well method where a tracer is forced out into the rock from a borehole section and, possibly after a waiting period, is pumped back into the borehole and the tracer recovery is measured. This type of test has been labelled with different names in the literature. Some of the most common names include *push-pull, huff-puff* and *single-well injection-withdrawal test (SWIW)*. In this report the term SWIW will be used, although this is not necessarily a recommendation.

In this report, existing literature about SWIW tests is reviewed with respect to practical feasibility and interpretation of transport processes. The review is restricted to SWIW tests in fractured rock, although the test method may also be applied to porous unconsolidated media. Further, scoping calculations are carried out for conditions expected under the site investigation programme. The purpose of the literature review is to provide basic background information for implementation of the method for Swedish bedrock conditions and also to provide background for the scoping calculations. The purpose of the scoping calculations is to provide further and more specific hydraulic background information for field implementation and to explore possibilities regarding interpretation of test results.

There are other single-hole methods not considered in this report. One example is the single-hole dipole tracer test /Sutton et al., 2000/. In this method, a flow dipole is created between two isolated sections in the same borehole and the in-flowing water is labelled with a tracer. Another single-hole tracer test method is the dilution test, which is used to determine the groundwater flow through a borehole section. Sometimes the

latter approach is combined with a pump-back period and is then at least partly a type of SWIW test.

The scoping calculations in this report are carried out with emphasis on using the dilution probe /Gustafsson, 2001/ as the primary equipment for SWIW tests in the site investigation programme. This has an obvious advantage because the same equipment may then be used for both flow measurements (by dilution tests) as well as SWIW tests. Other equipment designs are possible and the findings from the scoping calculations should be, generally, relevant for these as well.

2 General features of SWIW tests

2.1 Basic outline of a SWIW test

A SWIW test may consist of all or some of the following phases:

1. Injection of fluid to establish steady state hydraulic conditions.
2. Injection of one or more tracers.
3. Injection of chaser fluid after tracer injection is stopped, possibly also label the chaser fluid with a different tracer.
4. Waiting phase.
5. Recovery phase.

The waiting phase is sometimes also called the shut-in period or resting period.

The tracer breakthrough data that is eventually used for evaluation is obtained from the recovery phase. The injection of chaser fluid has the effect of pushing the tracer out as a "ring" in the formation surrounding the tested section. This is generally a benefit because when the tracer is pumped back both ascending and descending parts are obtained in the recovery breakthrough curve. During the waiting phase there is no injection or withdrawal of fluid. The purpose of this phase is to increase the time available for time-dependent transport-processes so that these may be more easily evaluated from the resulting breakthrough curve. A schematic example of a resulting breakthrough curve during a SWIW test is shown in Figure 2-1.

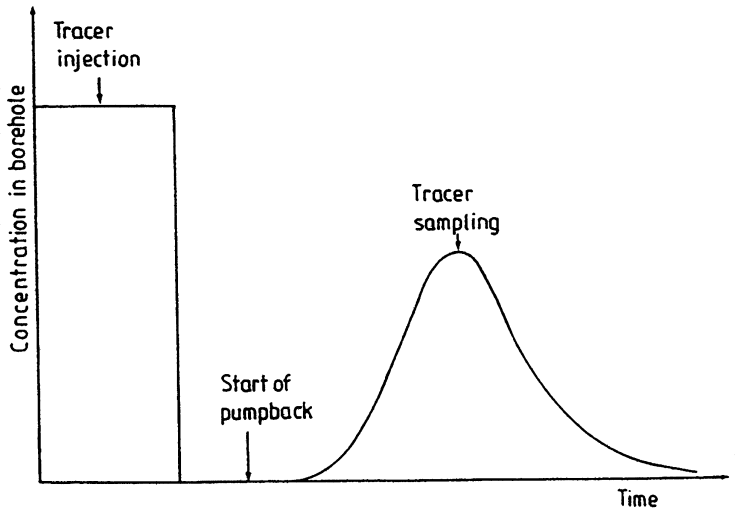

Figure 2-1. *Schematic tracer concentration sequence during a SWIW test /from Andersson, 1995/.*

The design of a successful SWIW test requires prior determination of injection and withdrawal flow rates, duration of tracer injection, duration of the various injection, waiting and pumping phases, selection of tracers, tracer injection concentrations, etc.

2.2 Limitations and possibilities

The performance of a SWIW test is, to different degrees, sensitive to the flow conditions and the rock properties. Such factors may be very important for a successful experimental design and will require careful consideration. A few common "problems" are listed and briefly discussed below. These and others will be discussed in more detail in subsequent sections.

Existing hydraulic gradient

An existing, or "natural", hydraulic gradient across the tested rock volume may be one of the most disturbing factors for a SWIW test. Such gradients will cause the injected tracer to drift away during the entire duration of the test. A significant gradient may make it difficult to pump back all, or any, of the tracer during the recovery phase. Prior knowledge of the magnitude of the gradient is likely to be very important for test design.

Heterogeneity of flow and transport properties

For tracer tests in general, it may be argued that effects of heterogeneity in the breakthrough curves might obscure effects of other processes. Heterogeneity may be an important factor also for SWIW tests. Although the reversibility of flow is a theoretical advantage for the SWIW test, the presence of a natural hydraulic gradient may, especially during the waiting phase, drive the solute through different flow paths than it would during the injection and recovery phases. In such cases, sufficient reversibility might not be obtained. This effect is also dependent on the location of the borehole section relative to the location of high-transmissivity flow paths.

Aspects of parameter identification and estimation

Because of the theoretical reversibility of flow, SWIW tests are generally considered suitable for interpretation of time-dependent processes, such as matrix diffusion. In the absence of a significant hydraulic gradient (see above), the flow field should be reversible even if the formation properties are spatially heterogeneous. Thus, SWIW tests would be advantageous, for interpretation of time-dependent processes, compared with multi-well tests.

On the other hand, other processes and parameters may be more difficult to identify/estimate compared with multi-well tests. For example, dispersivity values would be expected to be different (smaller) than the ones obtained from multi-well tests because the reversal of flow fields obscures the dispersion resulting from flow paths of different velocities. Using similar reasoning, it may also be expected to be more difficult, compared with multi-well tests, to estimate linear retardation coefficients (e.g. K_d-sorption).

3 Previous studies

This chapter describes a number a previous studies involving SWIW tests. The review describes studies one by one in an increasing order of complexity regarding experimental conditions and interpretation methods. The emphasis on this review is relevance to the site investigation programme, which results in more extensive descriptions of some of the references.

SWIW tests were first developed within the oil industry in order to estimate residual oil saturation in the rock /Tomich et al., 1973/ and this particular application was also patented in the U.S. 1971 /Deans, 1971/. The basic procedure in this application is to simultaneously inject a hydrophilic alcohol and an oil-soluble ester with the injected water. The ester will dissolve in the oil-phase, which is the immobile phase, and thus be retarded relative to the alcohol. During a waiting period (typically two to six days) some of the retarded ester (absorbed in the immobile oil phase) reacts and forms another hydrophilic alcohol. In other words, a new tracer is produced in the formation prior to the withdrawal phase. During the withdrawal phase, the two different alcohols arrive at different time in the borehole and the retardation may thus be quantified.

Early developments of the single-hole tracer testing in the field of geohydrology mostly concerned estimation of parameters such as porosity and dispersivities. A method wherein the fluid injection phase is replaced by natural outflow into the formation was presented by Borowczyk et al. /1967/ which was used to estimate porosity. A similar approach is also presented by Bachmat et al. /1988/. Methods to estimate longitudinal dispersivities from SWIW tests were presented by Mercado /1966/, Gelhar and Collins /1971/ and Fried /1975/.

The earliest studies assumed homogeneous single-layer aquifers. Extensions to single-well tracer tests in stratified aquifers with layers of different hydraulic conductivity, which would correspond to two or more conductive fractures in the same isolated borehole section, were presented by Pickens and Grisak /1981/, Güven et al. /1985/ and Molz et al. /1985/. Noy and Holmes /1986/ describe a multi-layered approach in a fractured formation featuring a double-packer system. A constant flow rate was used to inject tracer and the following chaser fluid. Dispersivity values were determined from the withdrawal phase breakthrough curve. Noy and Holmes /1986/ studied SWIW performance for a range of hydraulic conductivity values and suggested that the method is less applicable, mainly because of long test times, in formations with hydraulic conductivity values below 10^{-8} m/s.

It may be mentioned here, and which was pointed out by Gelhar et al. /1992/ that dispersivity values evaluated from SWIW tests should be expected to be different from values evaluated from other types of tracer tests when the formation is heterogeneous. In a heterogeneous (e.g. stratified) formation, the injected tracer will travel outward with different velocities during the fluid injection phases. However, when the flow field is reversed, the tracers will also travel with the same velocities back to the pumped section. Thus, dispersivity values obtained from SWIW tests are likely to be lower compared with estimates obtained from cross-hole tracer tests.

Bear /1979/ provides a relatively detailed discussion on the hydraulics of injection and withdrawal of fluid in a homogeneous single layer under an existing uniform hydraulic gradient. The SWIW method may be used to determine the existing gradient, as was presented by Leap and Kaplan /1988/ and Hall et al. /1991/. Nagra /McNeish et al., 1990/ estimated effective porosity and dispersivity, under an existing natural hydraulic gradient estimated from dilution measurements, from the recovery phase data of a SWIW test in the Lueggern borehole.

SWIW tests have also been used to study other solute processes than advection and dispersion. A few studies address the evaluation of sorption of solutes from SWIW recovery phase breakthrough curves. Schroth et al. /2001/ provides a relatively extensive discussion of the determination of sorption attributes for a few simple cases of equilibrium and non-equilibrium sorption in a radial flow system. Schroth et al. /2001/ demonstrates that, in the absence of hydrodynamic dispersion, linear equilibrium sorption (i.e. "K_d-sorption") of a solute may not be distinguished from a solute with no sorption. However, they also show that the presence of hydrodynamic dispersion will result in different recovery phase breakthrough curves for solutes with different linear retardation factors. A Langmuir sorption isotherm was used for non-linear equilibrium sorption and a first-order rate model for the non-equilibrium model. Some simulations were carried out in a layered formation, with different average water velocities in each layer. Drever and McKee /1980/ also used the Langmuir isotherm to evaluate adsorption parameters in a uranium formation using a SWIW test.

There are a number of studies that investigate time-dependent solute processes. In principle, SWIW tests should be especially useful for identifying and quantifying such processes. Snodgrass and Kitandis /1998/ presented a method to evaluate first-order and zero-order reaction rates from SWIW test. Haggerty et al. /1998/ performed a similar study with first-order reactions. Istok et al. /1997/ and Istok et al. /2001/ also considered zero-order, first-order and Michaelis-Menten type kinetics when studying microbial activities during SWIW tests.

Another important time-dependent process that has been studied with SWIW test is diffusion of solute into immobile regions (i.e. the rock matrix). Tsang /1995a, 1995b/ studied matrix diffusion effects and possibilities to identify this process in the presence of spatial heterogeneity. A comparison of SWIW tests, radially converging tracer tests and dipole tracer tests were made and the general conclusion was that the SWIW test is particularly suited for identifying matrix diffusion. Further, it was suggested in this study, which involved relatively high matrix porosity, that matrix diffusion can be identified even in the presence of extreme heterogeneity. This study considered a relatively porous matrix and a mean hydraulic fracture conductivity of approximately 5×10^{-6} m/s.

Haggerty et al. /2000a/, Haggerty et al. /2000b/ and Haggerty et al. /2001/ applied more elaborate models of rate-limited solute mass transfer to SWIW test tracer breakthrough data. They considered multiple-rate mass transfer between mobile and immobile zones. Variability in mass transfer rates may be expected because of variability in matrix block size, tortuousity, pore geometry, constrictivity and chemical sorption. In addition diffusion into dead-end pores and other immobile zones may contribute. The authors defined this variability using a statistical distribution.

The above-mentioned studies consider individual transport or formation attributes under relatively idealised conditions. For example, the studies involving various reactions often assume no regional gradient and homogeneous conditions. The studies considering heterogeneity assume no natural gradient, and so on. Only a few studies address the combined effects and how that affects the interpretation of the SWIW tests. Lessoff and Konikow /1997/ present a relatively thorough numerical simulation study of the combined effect of several factors on the interpretation of SWIW tests. In specific, they study how the combination of heterogeneity, natural gradient and hydrodynamic dispersion affects the possibilities of identifying/quantifying matrix diffusion. Their results suggest that the combination of heterogeneity and existing natural gradient may disturb the theoretical reversibility of SWIW tests and that experimental results are sensitive to whether the tested section happen to be located in a high- or low-permeability patch. It is also suggested that this combined effect may result in significant tailing in the recovery breakthrough curves and be confused with effect of matrix diffusion. Some guidelines are also suggested how to alleviate interpretation problems because of these combined effects, such as using multiple tracers, minimising the waiting period and performing multiple tests with different pumping schedules. The authors point out the trade-off between shortening the waiting time and allowing time for time-dependent processes (e.g. matrix diffusion). Experimental design for subsequent SWIW tests in the Culebra Dolomite /Meigs et al. (editors), 2000; Meigs and Beauheim, 2001/ were partly based on these results.

Lessoff and Konikow /1997/ used two different simulation models. One is a vertical cross-section with radial flow symmetry (thus, no natural hydraulic gradient) for studying matrix diffusion, where the matrix is modelled explicitly as layers with very low hydraulic conductivity. The other simulation model is a single-porosity heterogeneous layer with a natural gradient, with spatially correlated transmissivity. The results from the two models were compared to each other in order to identify under what conditions similar tracer recovery may be obtained. Thus, the effects of an existing hydraulic gradient and heterogeneity were not studied in a single simulation model in this case.

Altman et al. /2000/ extends the study of Lessoff and Konikow /1997/ by including matrix diffusion, heterogeneity and gradient in one simulation model. Altman et al. /2000/ also employed a single-porosity heterogeneous model with an existing gradient. They applied these models to SWIW data from the Culebra site /Meigs et al. (editors), 2000/ and concluded that breakthrough data could not be matched with the single-porosity model, even in the presence of heterogeneity and an existing natural gradient. The dolomite formation at this site has a high porosity and a moderate gradient. Based on their simulations, Altman et al. /2000/ suggest that the worst-case scenario for interpreting a SWIW test entails low porosity, high gradient and high heterogeneity. It is also recommended that tracers with the potential of several orders of magnitude of resolution in concentration should be selected, data should be collected over a long period of time to get several orders of magnitude in the tracer recovery breakthrough curve and that the data should be of high precision and accuracy.

The study by Altman et al. /2000/ and several other studies concern tracer tests in the Culebra Dolomite at the Waste Isolation Pilot Plant (WIPP) site in New Mexico. These tests include both SWIW and radially converging tests and are summarised by Meigs et al. (editors) /2000/. The transmissivity of this formation was found to approximately

range between 0.5 x 10^{-6} to 0.5 x 10^{-5} m/s. A relatively high matrix porosity of about 0.15 was also found.

Summary of literature review

Several of the above mentioned studies provide valuable background information for considering SWIW tests in the Swedish site investigation programme (PLU). However, experimental conditions in most cases are not directly comparable because the Swedish sites will likely show different flow conditions and formation properties compared with many of the available studies. The demands on experimental design will likely be different and possibly also higher. Scoping calculations are necessary prior to field implementation of the method at Swedish sites.

4 Requirements for implementation of SWIW for crystalline bedrock conditions

The depth range the method is expected to be applied to for the forthcoming site investigation programme (PLU) is about 300–700 metres. Several tracer experiments have previously been carried out in fractured rock in this depth range and the application of SWIW tests is not expected to introduce any new difficulties, with respect to large depths, compared to other types of tracer experiments.

The SWIW method is expected to be most effective in an intermediate range of transmissivity. A preliminary approximate range for application is postulated to be 1×10^{-8} to 1×10^{-6} m^2/s.

Another major factor for application of SWIW is the influence of an existing natural gradient. A SWIW test benefits from long waiting times, especially for evaluation of time-dependent processes (for example diffusion into the rock matrix). A desirable condition is, thus, that existing gradients are low. This likely means that the method may be expected to be of limited usefulness close to tunnels, shafts, or other hydraulic drains. However, in future site investigations relatively low gradients are expected. Values of hydraulic gradients obtained from dilution measurements in Swedish bedrock, without the presence of major artificial drains, range between very low values up to hydraulic gradients of the order of 2–3%. The scoping calculations are designed to provide an estimate of upper limits of feasible waiting times in the presence of expected natural hydraulic gradients.

It is anticipated that the SWIW tests are to be performed in boreholes with diameters of 56 or 76 mm in packed-off sections with a length of 1–2 m.

In this report, it is assumed that the main candidate for experimental equipment is the dilution probe /Gustafsson, 2001/. Any discussion in this report of experimental equipment requirements, limitations, etc, refers to use of the dilution probe. In principle, all phases of a SWIW test can be accomplished using this equipment. The main experimental constraints due to the equipment that must be considered in the scoping calculations are feasible pressures (during fluid injection and extraction phases) and feasible flow rates. Feasible pressures are about 5 bar (about 50 m head) and flow rates should range from about 25 to 300 ml/min. Another important issue is the dynamic range of tracer concentration that may be measured. The built-in measurement systems in the dilution probe may in some cases not provide sufficient dynamic range and then surface sampling and analysis may be employed instead.

5 Outline of scoping calculations

5.1 General

The main purposes of the scoping calculations are to:

- Determine the experimental constraints for expected ranges of field conditions.
- Investigate identifiability of flow and transport processes and parameters under ranges of expected experimental and field conditions.

The first aspect entails determination of appropriate experimental attributes such as:

- injection flow rate and tracer concentrations,
- chaser flow rate and duration,
- waiting time,
- withdrawal flow rate,
- selection of tracers.

These factors are necessary to control in order to successfully carry out an individual test. In order to ensure that the SWIW method is generally applicable for a wide range of field conditions, a relatively detailed study of these factors is needed.

The second of the purposes listed above concerns the overall goal of the method, which is to identify and quantify transport attributes of interest, such as:

- flow porosity (or equivalent),
- dispersivities,
- sorption coefficients,
- matrix diffusion coefficients.

The intention of the scoping calculations in this case is to investigate which and how many attributes may be identified and quantified under different experimental and field conditions. The scoping calculations are in this study limited to homogeneous conditions, while the impact of heterogeneity is discussed qualitatively in section 6.3.

5.2 Simulated scenarios

Although it is well known that fractures are heterogeneous, specific design for each individual test will, by necessity, likely be based on homogeneous assumptions. The information available prior to a SWIW test will likely be limited to a transmissivity value and the groundwater flow rate through the borehole section.

The simulations in this study include combinations of the following attributes:

Field flow conditions and rock properties:

Transmissivity:	10^{-6} and 10^{-8} m^2/s.
Flow porosity:	0.005 and 0.0005.
Natural gradient:	0 and 0.02

Experimental variables:

Injection flow rate:	3.5 to 700 ml/min depending on the transmissivity (corresponding to injection pressures ranging approximately from 5 m to 50 m).
Tracer injection length:	10–120 minutes.
Chaser duration:	10–20 hours.
Waiting time:	30–120 hours.
Extraction flow rates:	the same as for tracer injection and chaser fluid.

The simulations are intended to provide a sample of basic experimental scenarios that may be used to design an individual test. Primary features of a successful test are, for example, large tracer recovery (i.e. natural gradient vs. injection/pumping rates) and that complete breakthrough curves are obtained (i.e. both ascending and descending parts) within reasonable time frames.

For selected simulation scenarios, simple processes in the form of linear equilibrium sorption and diffusion into a stagnant rock matrix are included.

A brief study is also included whether it makes any difference from an experimental and interpretation point of view which method is used to inject/withdraw water from the formation. Further, it is considered whether it is important to account for transient flow effects in design and interpretation. Most scoping calculations in this study includes transient flow as well as transient transport unless it is determined that steady-state simulations give sufficiently good results. Nevertheless, it is appropriate to document any expected discrepancies that might arise if transient flow effects are ignored, as is common in studies of SWIW tests.

5.2.1 Sensitivity analysis for identification and quantification of flow and transport attributes

This section outlines how this analysis is carried out. Although the above sections describe scoping calculations for experimental feasibility, the identification of processes and parameters is relevant to all parts above also wherever appropriate. Basically, this section deals with the problem which and how many processes/parameters may be identified, and possibly quantified, from a SWIW test.

The basis for the analysis in this section is the calculation of parameter sensitivities. Parameter sensitivity is here defined as the partial derivative of a dependent variable (in this case concentration) with respect to each parameter. The sensitivity, x_{ij}, of parameter j at observation point i may thus be written as:

$$x_{ij} = \frac{\partial y_i}{\partial b_j} \tag{5-1}$$

where y_i denotes the independent variable (in this case concentration) at observation point i and b_j is the value for parameter j. It is often useful to scale the sensitivities to the value of the parameter:

$$x_{sc,ij} = b_j \frac{\partial y_i}{\partial b_j} \tag{5-2}$$

In this report, scaled sensitivities are used.

Parameter sensitivities may be plotted in various ways so that the sensitivity values may be examined in relation to the measurement points. Generally, high sensitivities are beneficial for identification/estimation of a parameter. By examining how the sensitivity varies in, for example, time one may identify which parts of the tracer breakthrough curve are useful for that particular parameter.

The parameter sensitivity is related to the estimation uncertainty of the various parameters. In common estimation approaches, such as non-linear regression, the parameter co-variance matrix, Cov(b), may be expressed as:

$$\mathrm{Cov}(b) = s^2(\mathbf{X}^T\mathbf{X})^{-1} \tag{5-3}$$

where $\mathbf{X}$ is a sensitivity matrix with one column for each estimation parameter and one row for each measurement, s^2 is the error variance:

$$s^2 = \frac{\sum_{i=1}^{n_o}(y_i^M - y_i^C)^2}{n_o - n_p} \tag{5-4}$$

where y_i^M and y_i^C denote measured and computed values, respectively, at observation point i, n_o is the number of observations and n_p is the number of parameters.

The parameter co-variance matrix contains the standard errors of estimation for each parameter in the diagonal and the co-variances in the off-diagonals. Prior to an experiment, s^2 is not available because there are yet no measurements. In such cases, relative estimation errors may still be used to compare different estimation scenarios. Another important piece of information in the co-variance matrix is the correlation between parameters. The linear correlation between any two parameters, p_1 and p_2, is given by:

$$r(p_1, p_2) = \frac{\mathrm{Cov}(p_1, p_2)}{\sqrt{\mathrm{Var}(p_1)\mathrm{Var}(p_2)}} \tag{5-5}$$

where the variance and co-variance terms are components of the $(\mathbf{X}^T\mathbf{X})^{-1}$ matrix. The correlation ranges between –1 and 1. Values close to either –1 or 1 indicate that a change in one parameter may be compensated for by a similar change in another to maintain the same fit between model and measurements. Correlation between parameters does not depend on the actual measurements, or the magnitudes of model errors, and may therefore be calculated in advance given an assumed set of parameter values

and a set of measurement locations (in time and/or space). The correlation between parameters may then be used to examine the identifiability of various parameter combinations and different experimental scenarios.

The sensitivity analysis results in information about the possibility of estimating a set of unknown parameter values from observed data. Specifically, the analysis in this report assumes that the entire tracer breakthrough curve from the recovery phase is used to fit the applied model employing some best-fit method such as regression. For further details and a review of similar design concepts, see Nordqvist /2001/.

Generally, the calculation of parameter sensitivities, and subsequently correlation and other diagnostic measures, is model-specific. Thus, different models may give different results depending on how the model is parameterised. Although only one general model concept is used here for the sensitivity analysis, the studied parameters appear in similar ways in other possible model concepts and the results should be generally applicable.

List of attributes that may be identified/quantified:

- porosity,
- dispersivities,
- magnitude of gradient (although this will normally be assumed to be available prior to the test),
- sorption coefficients (equilibrium processes),
- diffusion processes (non-equilibrium processes).

6 Scoping calculation results

6.1 Description of simulation model

The basic simulation code used for the scoping calculations is a modified version of the U.S.G.S. (United States Geological Survey) code SUTRA /Voss, 1984/. The basic model domain is a two-dimensional area, sufficiently large to decrease effects of model boundaries. The basic finite element mesh, which has a finer discretization around the well (0.2 x 0.2 m elements), is shown in Figure 6-1.

The simulations are generally carried out assuming both transient flow and transient transport during all phases. Although it may be possible during some phases to simplify conditions to steady state flow, transient simulations are generally employed because this does not present a significant computational inconvenience compared to steady state assumptions. In addition, there is no need to check that steady state flow assumptions will not have a significant impact on the simulated results. The numerical simulation is carried out in steps and a general simulation sequence for a SWIW test may be described as follows:

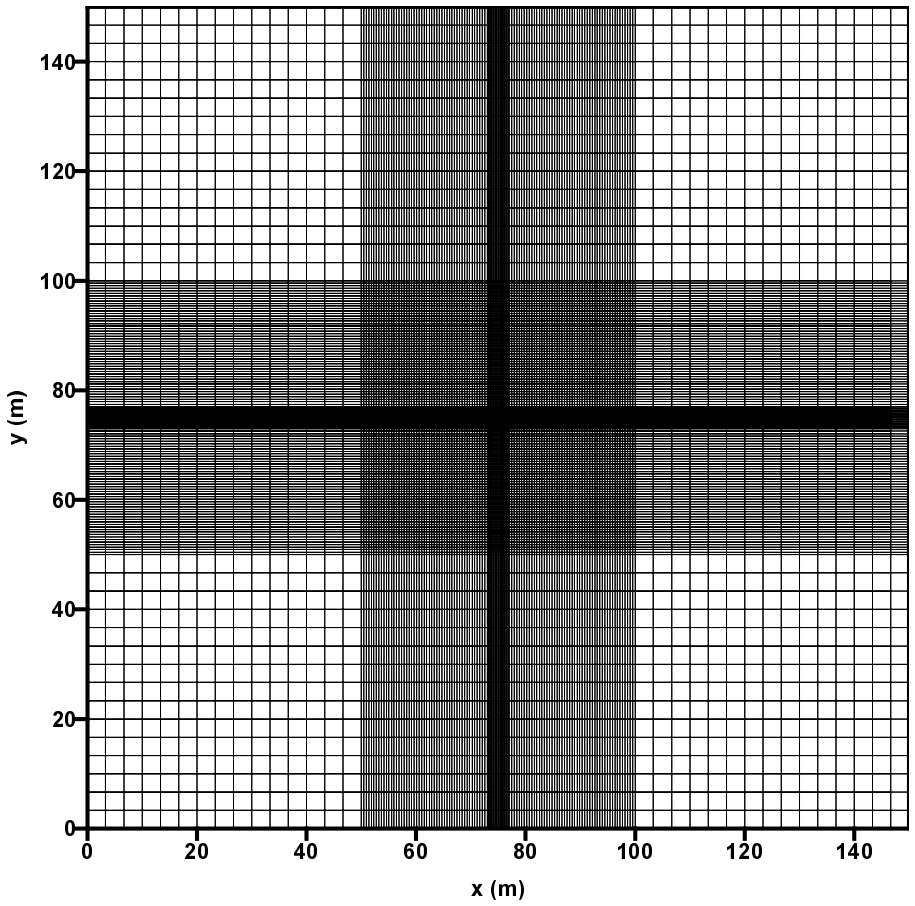

Figure 6-1. *Finite element mesh.*

1. Fluid and tracer injection phase. This may be done by assigning a constant head or a constant flow in the node representing the borehole section for the duration of the tracer injection. The tracer enters the formation with the in-flowing water. Generally, heads and concentrations are initially assumed to be zero everywhere in the model domain. A variant of this is to create steady-state flow conditions prior to the tracer injection.

2. Chaser fluid injection. This phase uses simulated conditions at the last time step for the previous phase as initial conditions. Fluid injection continues, generally at the same rate as in the previous step, but no tracer is included in the in-flowing water.

3. Waiting phase. Again, the simulated result from the end of the previous step is used as initial conditions. The boundary condition at the centre node, representing the test section, is removed for the duration of the waiting phase.

4. Extraction phase. The boundary condition at the centre node is again changed to constant flow (or constant head) except that water is now pumped back from the formation.

During all simulated sequences, a constant head boundary condition is set along the outer model boundary. Simulation time steps were chosen so they were very short whenever large changes occur during the simulation sequences (tracer injection phase, start of extraction phase, etc) and otherwise larger time steps were used. The chosen temporal and spatial discretization was found to give adequately low numerical errors. The discrepancy in the tracer mass returning to the borehole during the extraction phase compared with the total injected mass was generally found to be of the order of 1 percent or less.

The applied simulation model is based on an equivalent porous media approach. The specific values chosen for various parameters such as transmissivity, hydraulic conductivity, porosity, etc., are strictly valid only for this particular conceptualisation. For example, transmissivity and porosity should in this model be interpreted to be representative for the test section interval (generally assumed to be 1 meter in the simulations). Transmissivity is a measure of the total capacity of the section to conduct water flow, while the porosity gives a measure of the volume available for the flowing water. In other model conceptualisations, these and other parameters may be named and defined differently but the main mechanisms for flow and transport are likely to be very similar. Thus, the results from the scoping calculations in this report should have a large degree of generality. The choice of simulation model in this study is basically based on computational flexibility, numerical reliability and that it is a well-established code that continuously is updated and subject to extensive quality control.

Different parts of the simulation sequence are illustrated in the next section.

6.2 Numerical simulations of SWIW tests

6.2.1 Illustration of a simulation sequence

This section illustrates the different parts of a typical simulation sequence as an introduction to the procedure of a typical SWIW test. This example provides a more detailed illustration, compared with subsequent simulations in later sections, of flow and tracer behaviour during the different test phases. The following values of hydrogeologic parameters and experimental settings are used in the illustration example:

- Transmissivity = 10^{-6} m^2/s.
- Storativity = 10^{-5} .
- Porosity = 0.001.
- Longitudinal dispersivity = 0.5 m.
- Transverse dispersivity = 0.1 m.
- Tracer injection phase duration = 600 seconds = 10 minutes.
- Chaser injection phase end time = 36 000 s = 600 min = 10 h.
- Flow during injection, chaser and extraction phases = 5.8 x 10^{-6} m^3/s = 348 ml/min.
- Concentration of tracer in in-flowing water = 1.0.

The chosen values for the flow and transport properties are considered plausible for the intended type of experimental environment. The used flow rate is somewhat arbitrarily selected so that a significant, but well within the experimental equipment constraints, head change in the test section is obtained.

In this example a waiting phase is not included. Generally, a waiting phase is only considered in this study for cases with an ambient hydraulic gradient or time-dependent processes.

Hydraulic head

The simulated spatial distribution of hydraulic head at the end of the fluid injection phases (tracer injection and chaser phase) at 10 hours is shown in Figure 6-2. In this simple scenario, the result is the familiar cone shape resulting from a fluid injection in radial flow geometry. The main significance of Figure 6-2 is to illustrate the importance of the model boundaries on the simulated head contours. The outermost contour lines are clearly distorted by the boundaries and have a “square” appearance. However, at a radial distance of about 50 metres the contour lines are more or less perfectly circular. This distance is well beyond the area where tracer is expected to travel outwards during the simulated experiment. Therefore, the simulated tracer transport should not be significantly affected by the hydraulic model boundaries, i.e. effectively a radial domain for the transport simulations is created.

Hydraulic heads vs. time during the simulated test are shown in Figure 6-3. Because a relatively large storativity is used in the simulations, the transient effect on head values is relatively visible.

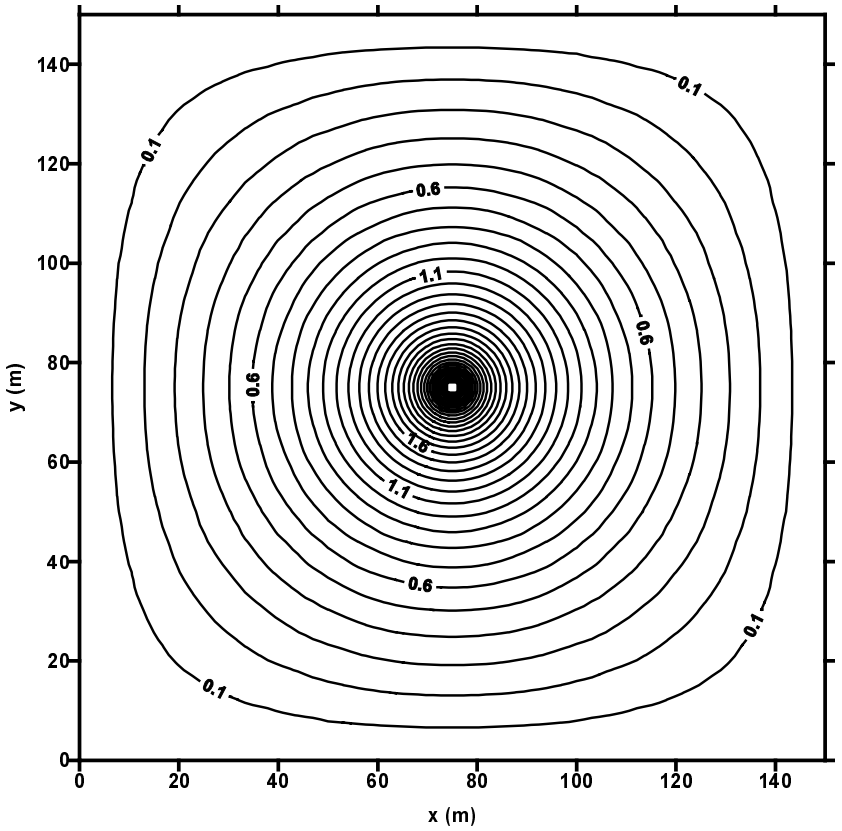

Figure 6-2. *Head distribution in a homogeneous domain at the end of the chaser injection phase.*

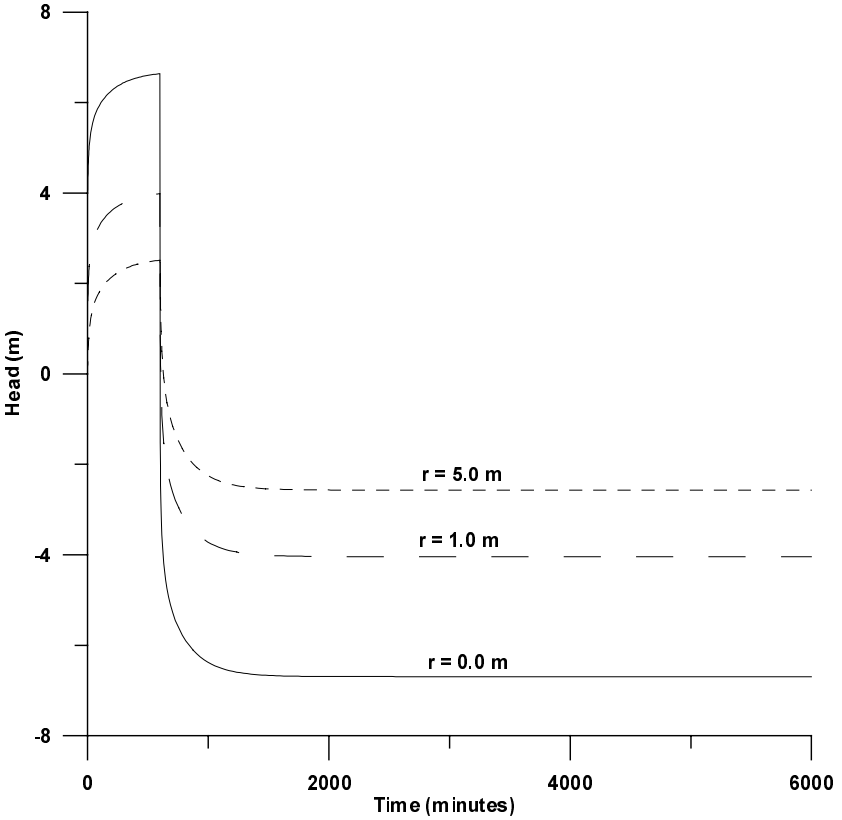

Figure 6-3a. *Simulated hydraulic heads vs. time in the test section (r = distance to the centre of the tested section) and nodes located 1 and 5 m away, respectively.*

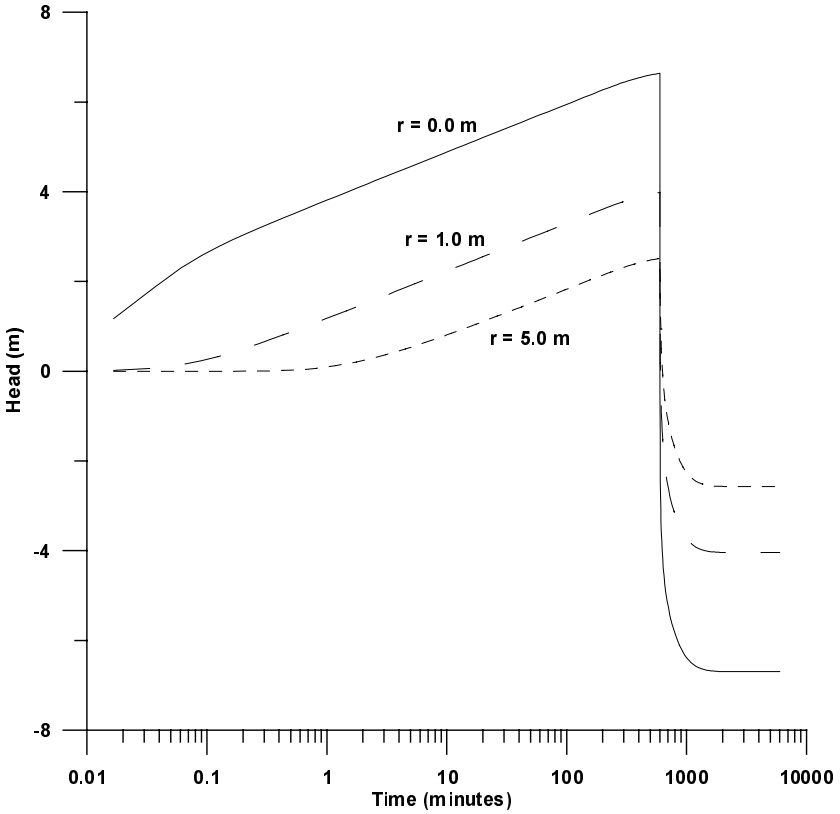

Figure 6-3b. *Simulated hydraulic heads vs. logarithmic time in the test section (r = distance to the centre of the tested section) and nodes located 1 and 5 m away, respectively.*

Concentration

A contour line plot of simulated tracer concentration at the end of the chaser injection phase (at 10 hours) is shown in Figure 6-4. The largest concentrations in the tracer "ring" is located about 8 metres from the injection node. The width of the ring is about 6 metres and, thus, the outer perimeter is located about 11 metres away from the centre.

A few plots of concentration vs. time are shown in Figure 6-5 for three different distances from the centre node. The curves for the nodes away from the centre node are shown mostly for an illustration of what happens away from the borehole and such information may not necessarily be available during actual site investigations. The primary measurements of tracer concentrations that will be made during site investigations correspond to the curve for r = 0.0 m in Figure 6-5d, which is the breakthrough curve for the tracer returning to the borehole during the extraction phase.

The resulting concentration levels (in terms of C/C_0) during the recovery phase are dependent on the total injected tracer mass, i.e. the length of the tracer injection period. In this case a relatively short injection period of 10 minutes is assumed, which results in a peak concentration in the recovery curve on the order of 1 percent ($C/C_0 \approx 0.01$). Longer injection periods may be employed if needed, which will result in higher recovery concentrations. Such considerations are mostly related to the dynamic range of the used tracer (i.e. the interval between the highest and lowest concentration, respectively, that may be measured) and will be important for the detailed design of actual field experiments.

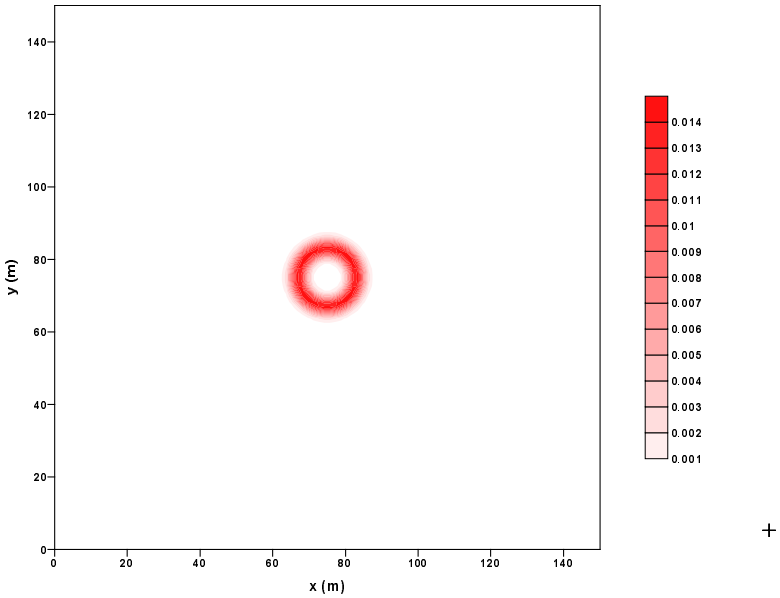

Figure 6-4. *Tracer concentration (relative to injection concentration) contours at the end of the chaser injection period.*

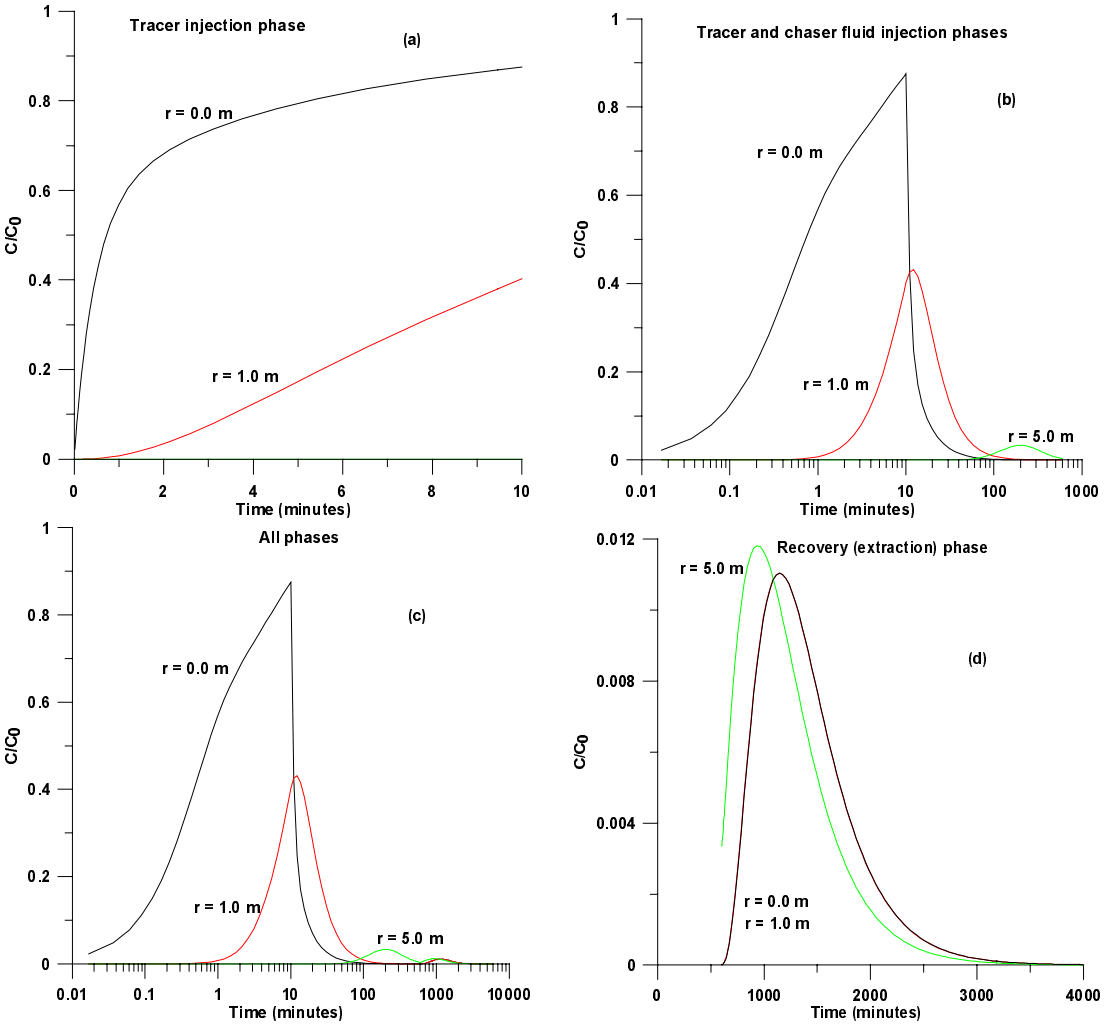

Figure 6-5. *Tracer concentration vs. time for a) tracer injection phase b) tracer and chaser fluid injection phases c) all phases d) recovery phase only. Indicated distances (r) are given as distance from the centre (injection) node.*

6.2.2 Constant head vs. constant flow as fluid injection method

One simulation was made in order to illustrate the difference between two different fluid injection methods. In the example in the previous section, a constant flow was applied. This is compared to an injection applying a constant head in the injection section. The applied head in the injection section is set to exactly the same steady-state head value as was obtained at the end of the extraction period in the preceding example. A comparison between the two methods is shown in Figure 6-6.

Figure 6-6 shows that resulting recovery breakthrough curves (Figure 6-6b) are similar in shape and temporal appearance. For the constant head case, somewhat more tracer mass is pushed out into the formation because of initial high flow rates when the head is raised instantaneously in the injection section. After one second, the flow into the formation is about 5–6 times higher than the steady-state flow. However, this is not a significant result with respect to experimental design issues because heads or flow may be set to any arbitrary value within the limits imposed by the equipment used. The main result here is that there are probably no particular advantages from a theoretical view-point which injection method is used. In this study, it is anticipated that the constant flow injection method is likely to be more feasible and this assumption will therefore generally be used in the simulations.

A potential issue related to the injection procedure is that, irrespective of the type of fluid injection, it will not be possible to obtain a distinct end of the tracer injection period. Instead, the injection of the tracer will decay exponentially at a rate depending on the volume of the borehole section. The potential negative effect of this would be that the ascending part of the tracer recovery curve becomes affected.

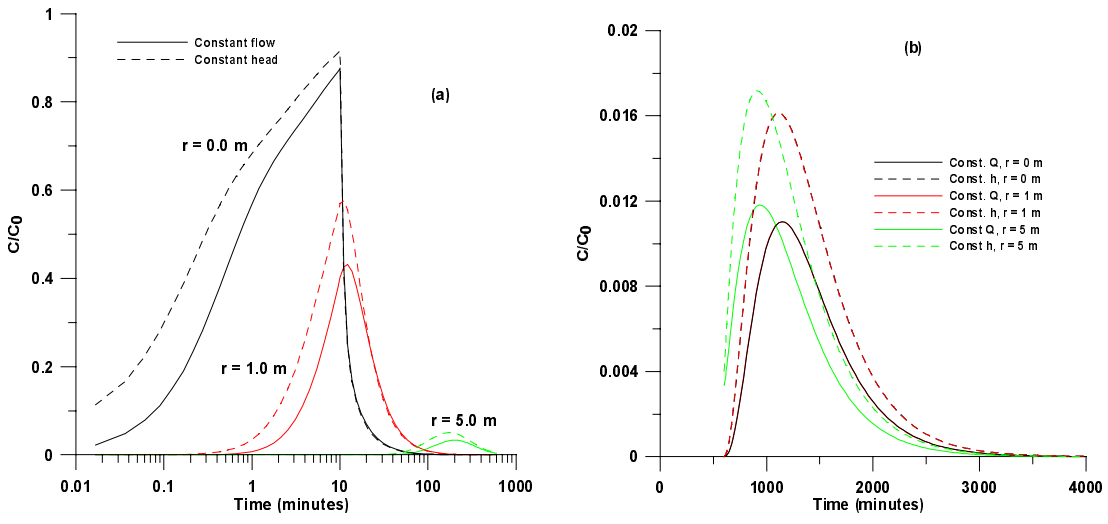

Figure 6-6. *Comparison of tracer concentration during the injection phase (a) and the recovery phase (b) between two different fluid injection methods.*

6.2.3 Transient vs. steady-state flow during injection phase

In general, the simulations in this report are carried out assuming both transient flow and transient transport. In order to briefly investigate the magnitude of any errors originating from neglecting transient flow effects (i.e. assume steady-state flow in all phases), the example in 6.2.1 was run assuming steady-state flow in each phase. A comparison is presented in Figure 6-7 showing very small differences in the resulting recovery breakthrough curves. Thus, one may, at least in this case, safely use the assumption of steady state flow. Such assumptions are especially convenient for standard evaluation approaches. However, for most of the simulations in this report transient flow is included simply because it is an unnecessary simplification and one does not need to regularly check the validity of steady-state assumptions. For other values of transmissivity and storativity, i.e. higher values of the hydraulic diffusivity (S/T), the transient effects may be larger and it may then be appropriate to check the validity of steady-state assumptions prior to analysis.

These results also imply that there are no obvious advantages (or disadvantages) of establishing a steady-state flow field prior to the tracer injection.

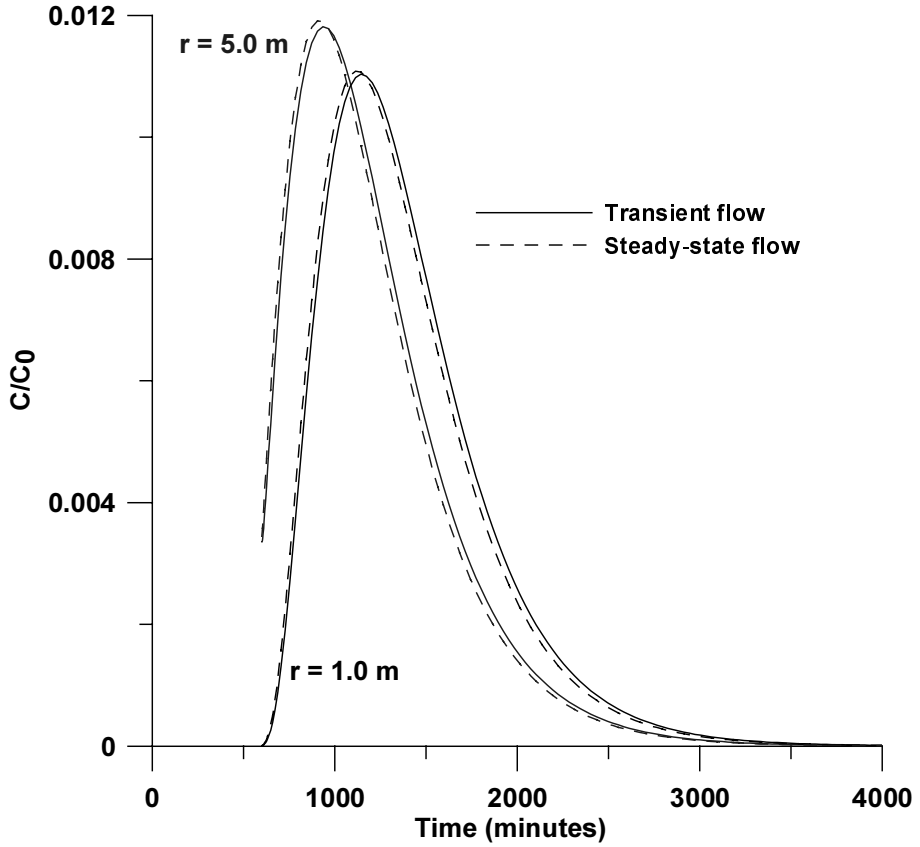

Figure 6-7. *Comparison of recovery (extraction phase) breakthrough curves for assumptions of steady state and transient flow, respectively.*

6.2.4 Simulations for ranges of expected flow conditions and rock properties

No hydraulic gradient

Scoping simulations without an ambient hydraulic gradient comprise the most basic experimental design information. For moderate values of aquifer storativity, as in the illustration example above, steady state flow conditions may be used as a preliminary assumption for a few simple initial calculations.

The steady state head at constant injection of fluid in a well, h_w, in a homogeneous confined aquifer may approximately be estimated from (in the absence of skin and other well factors):

$$h_w = \frac{Q}{2\pi T} \ln \frac{r}{r_w} + h \qquad (6\text{-}1)$$

where h is the head (m) at a radial distance (m) of r, r_w is the well radius (m), Q is the injection flow (m^3/s) and T is the transmissivity (m^2/s). Using the simulation domain described above, one may choose a reference head of h = 0.0 m at an approximate radial distance of r = 75.0 m. For these boundary conditions and an assumed well diameter of 0.076 m, the well head is plotted against transmissivity for a few different flow rates in Figure 6-8. The upper limit of the injection head for the considered test equipment is approximately 50 m, which is indicated by a horizontal line in the Figure 6-8. This limit indicates that at low T-values one should expect that restrictions apply to what flow rates may be selected. In this case, it appears that at the lower end of the considered transmissivity range (10^{-8} m^2/s) the flow rate of 35 ml/min approximately is a "limiting" flow rate.

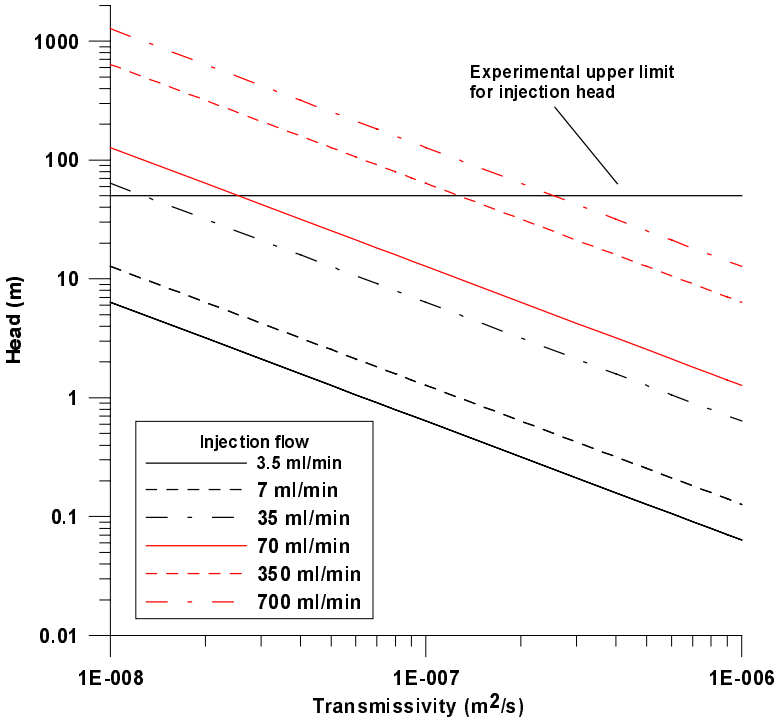

Figure 6-8. *Steady state head in injection well vs. transmissivity for different injection flow rates. The horizontal line indicates the upper limit (50 m) for the proposed test equipment.*

For the simulation geometry and chosen boundary conditions, transient tracer transport at steady state flow conditions only depend on the radial velocity distribution:

$$v(r) = \frac{Q}{2\pi rbp} \tag{6-2}$$

where v is the average water velocity (m/s), b is the aquifer thickness (m) and p the porosity (dimensionless). The thickness, b, may be thought of as the borehole section width and is in all simulations here set to a value of 1.0 m. A plot of the velocity vs. radial distance (calculated from eq. 6-2) is shown in Figure 6-9 for three different values of Q/bp. The Q/bp values represent in this case a maximum, a minimum and a "limiting" value. The maximum and minimum values, respectively, are obtained by using the assumed ranges of possible flow rates (3.5 and 700 ml/min) and porosity values (5×10^{-4} and 5×10^{-3}). The middle "limiting " case" represents a flow rate of 35 ml/min, which is the highest possible at $T = 10^{-8}$ m^2/s, and a porosity of 5×10^{-3}.

One may also illustrate the radial distance an injected tracer particle travels as a function of time, by the following relation:

$$r = \sqrt{\frac{Qt}{\pi bp} + r_w^2} \tag{6-3}$$

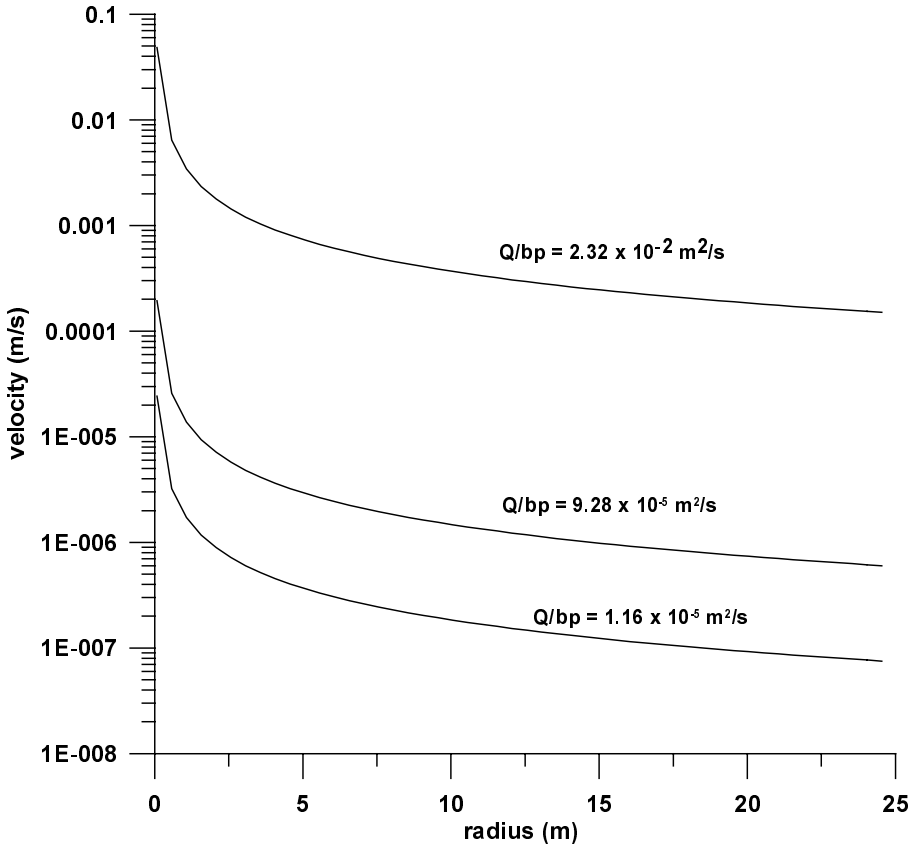

Figure 6-9. *Velocity as a function of radial distance for different values of Q/bp.*

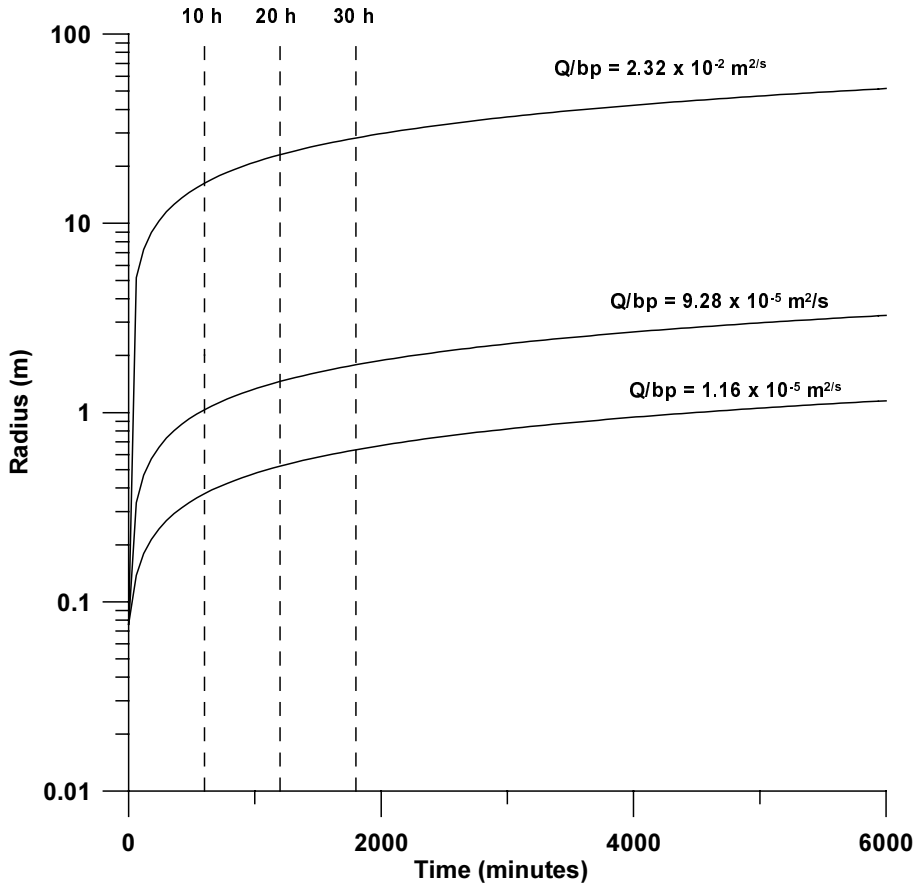

***Figure 6-10**. Radial travel distance for different values of Q/bp.*

A plot of radial travel distance vs. time based on eq. 6-3 is shown in Figure 6-10, where injection times for 10, 20 and 30 hours, respectively, are indicated with dashed lines.

The tracer transport is only dependent on the radial velocity distribution and other possible attributes such as dispersion. With the boundary conditions employed (i.e. constant injection of fluid with constant concentration) and the assumption of steady state flow, the resulting recovery breakthrough curves depend only on, besides dispersion and other processes, the injection and extraction flow rates, porosity and thickness. In axi-symmetric radial flow, the governing equation for solute transport with dispersion may be given as /Lee, 1999/:

$$\frac{a_L B}{r}\frac{\partial^2 C}{\partial r^2} - \frac{B}{r}\frac{\partial C}{\partial r} = \frac{\partial C}{\partial t} \qquad (6\text{-}4)$$

where $B = Q/2\pi pb$, a_L is the radial (longitudinal) dispersivity (m) and C is the concentration.

Figure 6-11 shows simulated breakthrough curves (using the numerical model described above) for a range of Q/bp values. The total range of Q/bp values is the same as in the preceding plots. Figure 6-11 summarises the range that may be expected for the expected limitations of the test equipment and the considered porosity range. Figure 6-11 shows that for low values of Q/bp (i.e. low velocities) recovery breakthrough

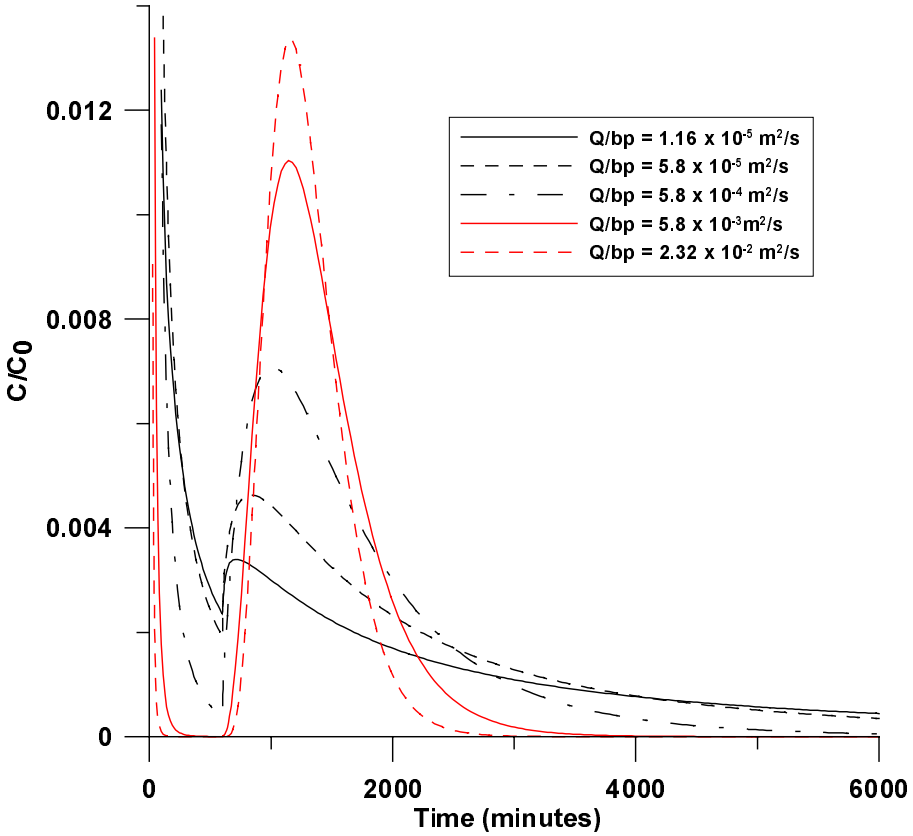

Figure 6-11. *Simulated tracer recovery curves for different values of Q/bp.*

curves become less distinct than for high values of Q/bp. The ascending part of the recovery is incomplete (does not start from zero) for several of the cases and is almost missing for the lowest value of Q/bp. In these cases, the tail of the breakthrough curves are also more extended and, thus, one would expect an increased time for the duration of the experiment.

Figure 6-11 indicates that it would be desirable to use high injection and extraction flow rates, especially considering that prior knowledge of the porosity (or some other representation of fracture volume) may not be available or only approximately known from other measurements. At the lowest considered transmissivity value ($T = 10^{-8}$ m^2/s), Figure 6-8 indicates that the highest permissible flow rate, to avoid excessively high injection pressures, would be around 35 ml/min. This flow rate, together with the highest value in the assumed porosity range, provides a limiting case of the lowest Q/bp (i.e. lowest velocity) value. The limiting case may be thought of as a "worst case" because it would illustrate the most incomplete breakthrough curve possible (i.e. missing some of the ascending part).

The choice of fluid injection and pumping rates must be made with care because the porosity (or some other measure of the volume available to flow) will, at best, only be approximately known beforehand. A high flow rate may result in that the tracer is being pushed too far out and may then also enter other connecting fractures. Low flow rates may, on the other hand, result in only a very small volume being tested. This problem may be alleviated with a strategy involving repeated experiments, although this would increase the total experimental time.

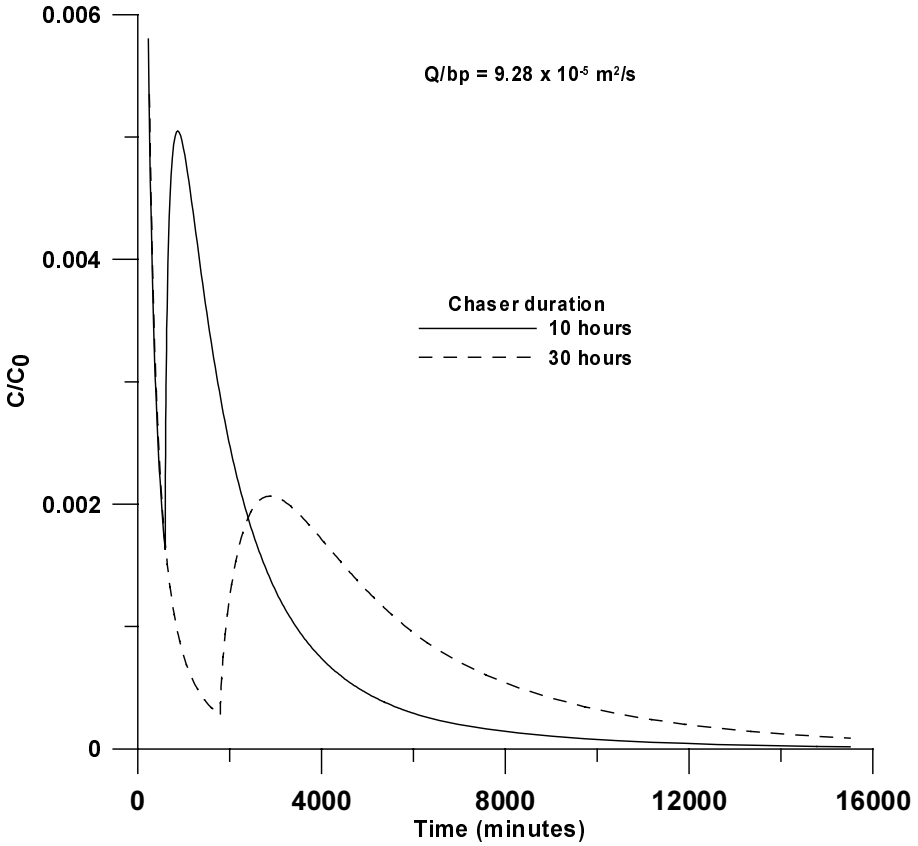

Figure 6-12. *Effect of chaser duration for the limiting case.*

The limiting case (Q = 35 ml/min, p = 5 x 10^{-3}) is shown separately in Figure 6-12. In addition, the remedial effect of using longer chaser duration is illustrated as well. In this case, the chaser duration is increased from about 10 hours to about 30 hours. The effect of extending the chaser fluid injection is that a more complete recovery breakthrough curve is obtained. This also results in lower peak concentrations and a longer breakthrough curve tail. Thus, the longer chaser duration puts higher demands on dynamic ranges of tracers and also requires longer experimental times. In this example, monitoring the breakthrough curve until about one percent of the peak concentration would require about 10 days.

The advantages of increasing the chaser duration are to obtain more distinct ascending part of the recovery curve and to access a larger volume of the tested feature. From Figure 6-10 one may estimate the radial travel distance to increase from about 1 metre to about 2 meters for this particular case.

It should be noted here that, in the scoping simulations, transmissivity and porosity values have been combined without any consideration to their relationship. It would in fact be reasonable to expect some, although there appears to be no straightforward method to determine it, relationship between T and p (e.g. the so-called cubic law). Larger porosity (i.e. fracture aperture) should result in larger T-values. The simulations here sometimes use combinations of low transmissivity with high porosity and vice versa as extreme conditions. Field situations may be expected to exhibit more favourable conditions and it is therefore possible that the present analysis is somewhat conservative. Thus, field feasibility of the SWIW method should be at least as favourable as in this analysis.

Hydraulic gradient

The effect on tracer recovery from the presence of a hydraulic gradient is simulated with the assumption of a uniform gradient across the simulation domain. In a uniform flow field, and in the absence of pumping, the drift (d) that takes place in a certain amount of time (t) may be calculated from:

$$d = \frac{T}{bp}\frac{dh}{dl}t \qquad (6\text{-}5)$$

where l denotes the direction of flow.

Figure 6-13 shows the drift vs. time in uniform flow field calculated from eq. 6-5 by employing a gradient of 2% (the assumed upper limit). A comparison with Figure 6-10 indicates that displacement due to a high gradient may be roughly on the same order of magnitude as radial travel distance due to pumping only. Thus, in the presence of a strong hydraulic gradient, it would be expected that tracer recovery may be significantly affected.

The position of the solute front, with injection radial flow, a uniform gradient in the x-direction and no dispersion, at a dimensionless time τ_0 may be expressed in dimensionless spatial variables ξ and η as /Bear, 1979/:

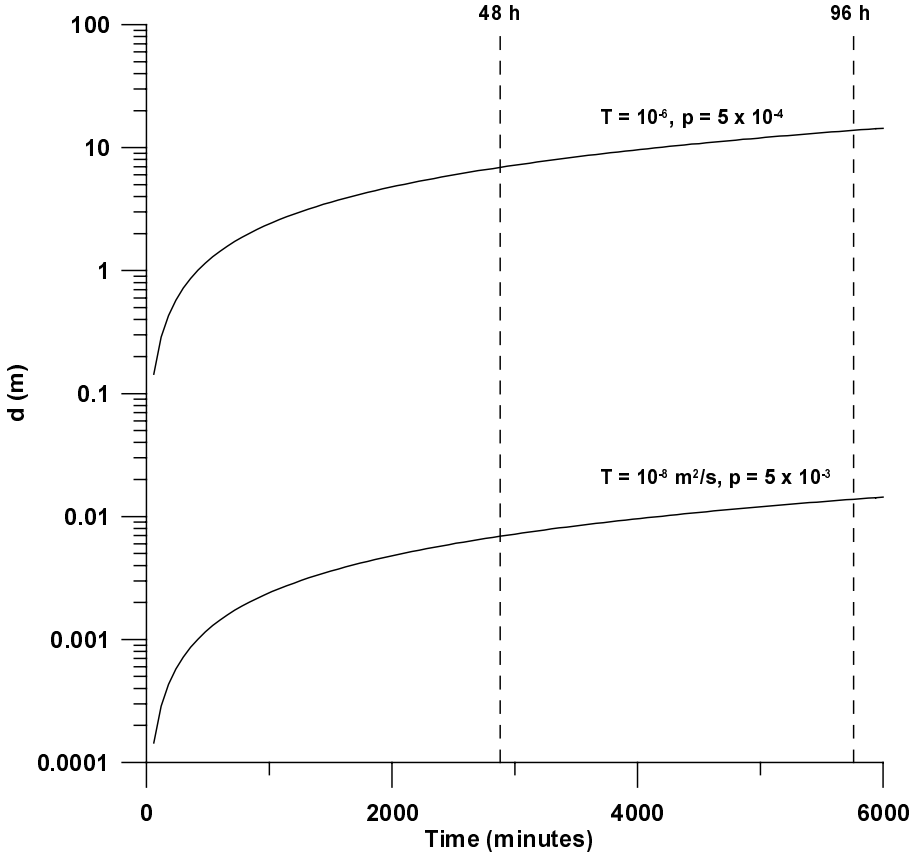

Figure 6-13. *Drift (d) as a function of time for extreme combinations of transmissivity and porosity. The gradient is assumed to be 2%. The vertical dashed lines provide an example what may be considered typical experimental time frames.*

$$\left[\cos\eta + \frac{\xi}{\eta}\sin\eta\right]\exp(-\xi) = \exp(-\tau_0) = \text{const.} \qquad (6\text{-}6)$$

where

$$\xi = \frac{2\pi q_0 b}{Q}x \qquad \eta = \frac{2\pi q_0 b}{Q}y \qquad \tau = \frac{2\pi q_0^2 b}{Qp}t$$

where x, y and t are the dimensional spatial co-ordinates, Q the injection flow rate (m^3/s), b is thickness (m), p is porosity and q_0 is the specific discharge (m/s) which is uniform in the x-direction. The variable q_0 is related to the gradient by:

$$\frac{dh}{dl} = \frac{bq_0}{T} \qquad (6\text{-}7)$$

The corresponding fronts for the recovery phase are obtained by taking the mirror image of the above with respect to the x-axis (or η-axis in dimensionless variables). An illustration of eq. 6-7 (using dimensional variables) is given in Figure 6-14, which shows a combination of variables that will give a relatively large effect of the gradient on tracer recovery. Such combinations involve large values of transmissivities and gradients together with a low value of porosity and moderate pumping rates. Figure 6-14 is based on T = 10^{-6} m^2/s, p = 5 x 10^{-4}, dh/dl = 0.02, Q = 350 ml/min and a chaser duration of 10 hours.

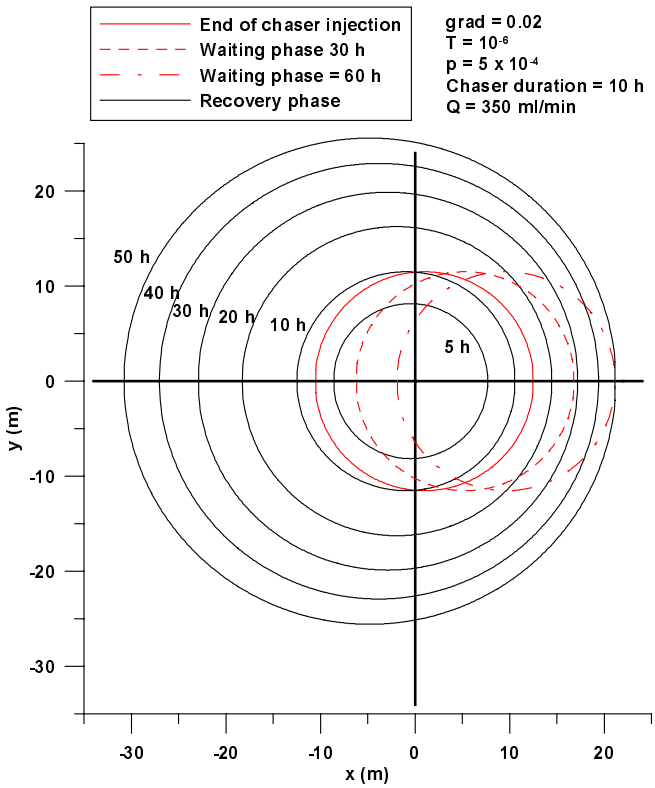

Figure 6-14. *Advective fronts at end of chaser injection, after two different waiting times (30 h and 60 h) and different extraction (pumpback) times.*

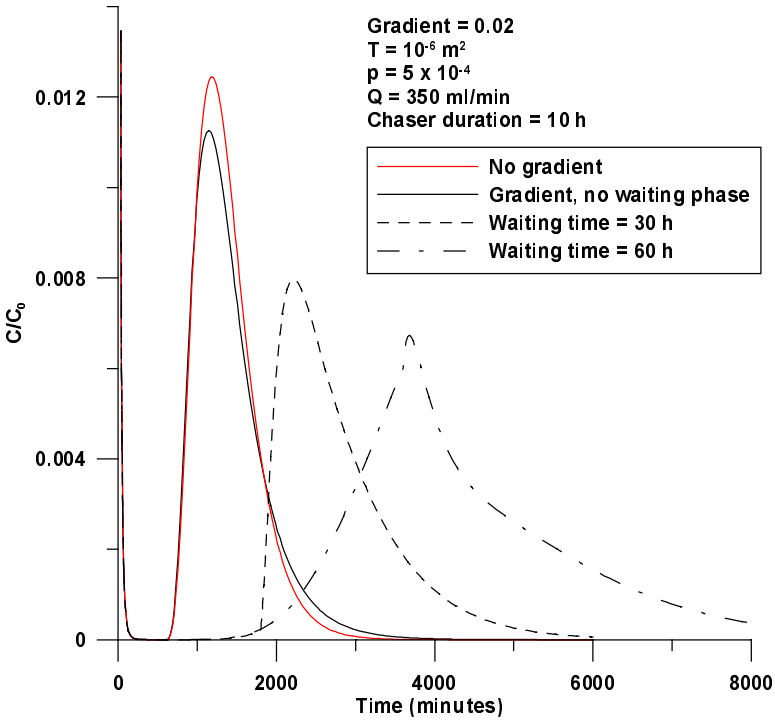

Figure 6-15. *Simulated breakthrough curves for the cases corresponding to Figure 6-14 with three different waiting times.*

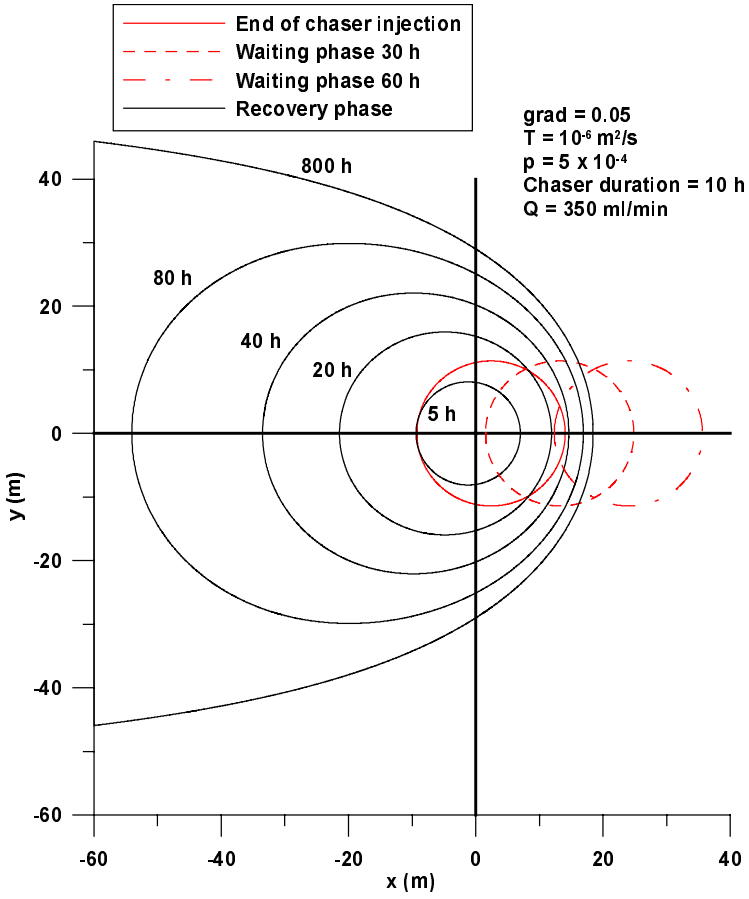

Figure 6-16. *Advective fronts for a background hydraulic gradient of 0.05.*

In Figure 6-14 the solid red line shows the advective front after a total time of fluid injection of 10 hours. This front is nearly circular and slightly elongated in the flow direction (x-direction). The black solid lines represent different advective fronts captured at different pumpback times during the recovery phase. At five hours of pumping, the black pumpback circle is completely within the red solid injection circle, which means that only water originating from the injected water is recovered. At ten hours of recovery, part of the pumpback circle is outside the injection circle, which means that the pumped water has begun to be a mix of injected water and original formation water. At 20 hours recovery, all the injected water is recovered and only original formation water is pumped.

The advective front after a waiting phase, represented by red dashed lines in Figure 6-14, is obtained by simple translation in the x-direction. With increasing waiting phase times, the tracer recovery during the fluid extraction phase is, for this case, significantly delayed. In addition, mixing characteristics over time are significantly changed and the time for complete recovery increases. For example, for the case with a waiting time of 60 hours, the time for complete recovery is about 120 hours (10 h fluid injection + 60 hours waiting time + 50 hours pumping time).

Breakthrough curves corresponding to the cases in Figure 6-14 were simulated with the numerical simulation model and are shown in Figure 6-15. The breakthrough curve for the case with no background hydraulic gradient is shown as well. The effect of including a waiting phase is generally to delay recovery but also to decrease the peak concentration in the breakthrough curve. The case with a waiting phase time of 30 hours results in a relatively simple shift in the recovery breakthrough curve. On the other hand, for the case of 60 hours waiting time the shape of the entire breakthrough curve is significantly affected by the hydraulic gradient. In fact, most of the ascending part of the tracer recovery curve for the latter case is caused by tracer returning to the borehole by the ambient flow during the waiting time. This is also illustrated in Figure 6-14 where parts of the advective front after 60 hours waiting times are close to the borehole.

In the preceding case, complete recovery could be expected even when assuming a gradient of 0.02. The above case may roughly represent a field situation where the impact of a natural gradient would be expected to be significant, with respect to field and experimental limits. Thus, implementation of the method should be practically feasible irrespective of the actual field conditions. However, at conditions where the importance of a background hydraulic gradient is substantial, some limitations may apply to the chosen duration of the waiting phase.

Advective fronts for a case with a higher background hydraulic gradient are shown in Figure 6-16. The gradient is set to 0.05 in this case, which may represent a plausible value in the vicinity of a tunnel or shaft.

Figure 6-16 indicates that substantial pumping times may be required in this case. In addition, when a waiting time is included, a substantial part of the injected tracer may never be recovered because the tracer has drifted beyond the hydraulic stagnant point “downstream” the pumped borehole. The advective front for 800 hours of pumping may, for practical purposes, essentially represent the hydraulic stagnation point in this case. Any tracer that travels beyond this point during the fluid injection and waiting phases may never be recovered during the fluid extraction phase.

The examples involving a uniform hydraulic background gradient in this section are based on the assumption that identical injection and extraction flow rates are used. For field implementation of the method, however, there are no requirements that flow rates are equal. Any flow rate (within constraints of the equipment) may be used during the different phases. There are a number of considerations that apply when choosing flow rates. Large injection flow rates will result in a larger volume tested, but may also require longer total experimental times. On the other hand, one might wish to restrict the injection flow to avoid having the tracer pushed out too far into the tested feature or decrease the risk that the tracer enters other fractures. Due to constraints imposed by acceptable pressures that may be handled by the proposed equipment, it appears likely that it would be advantageous to maximise injection flow at low values of transmissivity. At high transmissivities, on the other hand, one may want to restrict flows in order to prevent the tracer from travelling too far away from the borehole. With the considered experimental equipment, possible extraction rates are likely less than possible injection flow rates. However, in an actual field situation it may be desirable to use larger extraction flow rates than injection flow rates to ensure good tracer recovery, especially in the presence of a significant hydraulic gradient.

In a field situation, it is anticipated that transmissivity values for the tested section as well as flow measurements from dilution tests are available in advance. Thus, it is possible to identify possible flow rates and potential impact from the hydraulic gradient, and to choose experimental variables (chaser duration, waiting time, flow rates, etc.) for each individual SWIW-test. For example, the influence of a high gradient may be expected to be most significant at high transmissivity values. A suitable experimental strategy may be to reduce, or not include at all, the waiting time under such conditions. Identification of time-dependent processes will benefit from long waiting times, but it may be most useful to limit tests with long waiting times to features with low transmissivity or low hydraulic background gradient.

Although a high gradient may significantly affect tracer recovery breakthrough curves, this should not cause interpretation problems as long as the magnitude of the gradient can be measured independently. However, any employed interpretation model must account for the effects of the gradient.

6.2.5 Sensitivity analysis – Identification and quantification of processes

General

The sensitivity analysis in this section is carried out using the methods outlined in section 5.2.1. A related sensitivity analysis concerning SWIW test was also carried out by Haggerty et al. /2000/. The herein-employed simulation model defines the parameters studied. This means that the sensitivity analysis shows what would happen if the model used here is employed to estimate parameters from an experimental breakthrough curve. The analysis assumes that the entire tracer recovery breakthrough curve is used for parameter estimation, employing some best-fit procedure such as regression analysis. It should be noted that many alternative models might be equally valid as interpretation tools for experiments like SWIW tests. For example, porosity may be expressed as fracture width or volume in other conceptual models. Nevertheless, the simulation model used here captures the essential features of flow and transport in very similar

ways as alternative models and any conclusions should be generally valid and easily transferred to other conceptual models.

The parameter identification study is roughly divided into two parts. One concerns the identification of "advective" parameters such as porosity and dispersivity, while the other part considers the identification of processes such as linear equilibrium sorption and diffusion into a low-permeability porous matrix.

Porosity and dispersivity

The sensitivity analysis was carried out using a single set of parameter values, which were as follows:

Porosity = 0.001.

Thickness = 1.0 m.

Transmissivity = 10^{-6} m^2/s.

Longitudinal dispersivity = 0.5 m.

Transverse dispersivity = 0.1 m.

Initially, a basic sensitivity study was carried out involving only the porosity and dispersivities as estimation parameters. The sensitivities were calculated for the entire tracer recovery phase. Thus, it is assumed that frequently made measurements are available for the duration of the recovery phase. The behaviour of the sensitivity (plotted as scaled sensitivity) for porosity (p) and longitudinal dispersivity (a_L) is given in Figure 6-17. Figure 6-17 shows that both parameters have some sensitivity during most of the recovery curve (in the absence of dispersion, porosity will always have zero sensitivity). The magnitudes of the scaled sensitivities are relatively low, but probably enough in order to obtain a fairly reliable estimate if sample and analytical errors are low.

If both parameters are to be estimated simultaneously, it is also necessary that the correlation between the parameters is not excessively high. A visual inspection of Figure 6-17 indicates that the sensitivity curves for p and a_L appear to be in phase with each other and therefore one might expect the two parameters to be highly correlated. The co-variance matrix for this estimation scenario shows that, indeed, the correlation between p and a_L is 1.0. Thus, these two parameters are perfectly correlated and may not be estimated simultaneously from the tracer recovery curve. Although a change in either porosity or dispersivity will change the recovery breakthrough curve, either parameter change will change the breakthrough curve in exactly the same way. Either of the parameters may only be identified if the other is independently known. Alternatively, only the ratio of the two parameters may be estimated. In previous studies that have addressed these parameters, the porosity is usually assumed known from other measurements and then the dispersivity has been obtained from the tracer recovery curve. The fact that porosity and longitudinal dispersivity can not be estimated simultaneously is a limitation of SWIW tests compared to cross-hole tracer tests.

Transverse dispersivity has, of course, zero sensitivity at all times in this case because of the radial symmetry and homogeneous conditions.

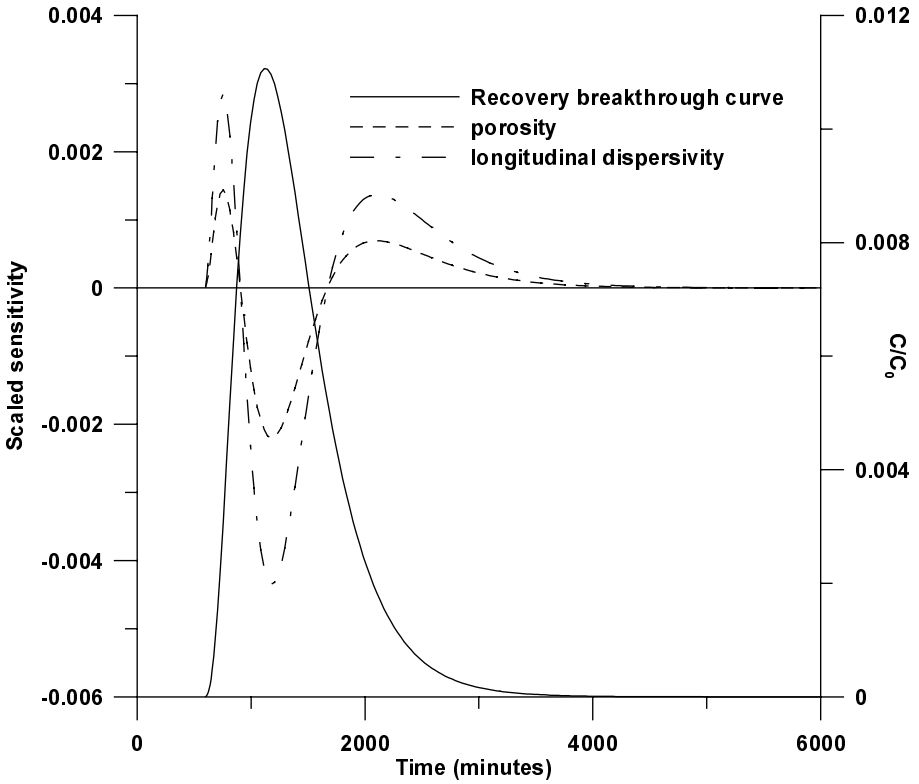

Figure 6-17. *Scaled sensitivity for porosity and longitudinal dispersivity.*

In the case where a significant hydraulic background gradient occurs, sensitivity behaviour differs from the preceding case. Assuming a gradient of 2%, a waiting phase duration of 30 hours and other parameter values as above, the sensitivity behaviour of porosity (p), longitudinal dispersivity (a_L), transverse dispersivity and the hydraulic gradient (g) is shown in Figure 6-18. In this figure, the sensitivity curve for longitudinal dispersivity is still similar to the corresponding one in Figure 6-17. However, the sensitivity to porosity behaves significantly different and is approximately a mirror image of the corresponding curve with no hydraulic gradient. A visual inspection of the two curves together (p and a_L) gives the impression that these two parameters may be more moderately correlated in this case. From the parameter co-variance matrix for the estimation scenario with only porosity and longitudinal dispersivity as estimation parameters, the correlation in this case turns out to be about 0.85. This is quite a moderate correlation value and indicates that these two parameters are possible to identify and estimate simultaneously from the tracer recovery curve in the presence of a background hydraulic gradient. Thus, this is a significant difference from the case with no hydraulic gradient where it is literally impossible to estimate p and a_L simultaneously from the tracer breakthrough curve. This is very clearly shown by the sensitivity analysis and may have implications for the field application of SWIW tests.

As postulated earlier, long waiting phase duration, and possibly also long chaser injection duration, is generally beneficial for identification of time-dependent processes. On the other hand, in the presence of a significant hydraulic gradient long waiting times may not be possible because of excessive plume drift. Thus, for estimation of the "advective" parameters p and a_L, the presence of a gradient is beneficial while identification of time-dependent processes may require the absence of a significant gradient. Thus, it is quite possible that parameter identification objectives for each test will have

to be adjusted according to ambient hydraulic conditions. Prior measurements of transmissivity (by hydraulic injection tests, for example) and ambient flow (by dilution tests) will provide the required background data for such considerations.

In Figure 6-18, sensitivity curves for the transverse dispersivity (a_T) and the hydraulic gradient (g) are also shown. The sensitivity behaviour of a_T is likely mostly only of theoretical interest, but one can nevertheless see that a_T has a small effect when the tracer plume is drifting. Thus, it is theoretically possible to estimate this parameter as well. Of more practical interest is the potential estimation of the hydraulic gradient directly from the recovery tracer curve (although dilution measurements also will give a prior estimate of the gradient). However, the parameter co-variance matrix assuming an estimation scenario with p, a_L and g estimated simultaneously show that all three parameters are highly correlated to each other and that this parameter combination is not possible to estimate. If the porosity would be assumed known, the gradient may be possible to estimate although the co-variance matrix for this case (simultaneous estimation of p and g) show that these parameters are somewhat highly correlated.

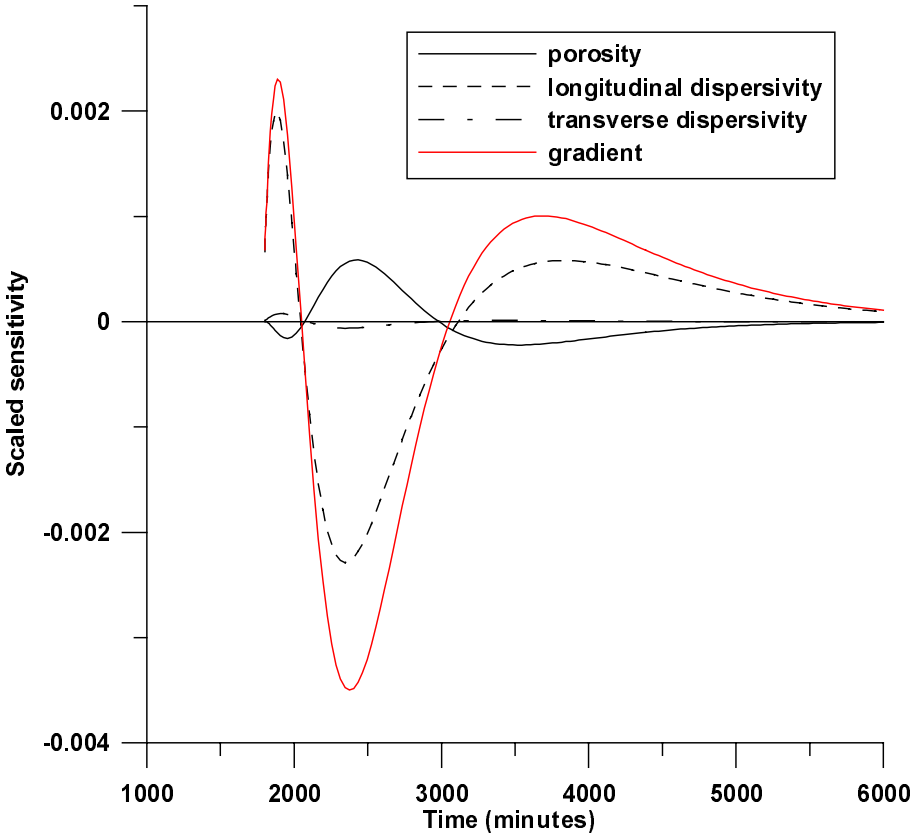

Figure 6-18. *Sensitivity behaviour assuming a gradient of 2% and waiting phase duration of 30 hours.*

Tracers affected by equilibrium sorption

For tracers that undergo linear equilibrium sorption ("K_d-sorption"), breakthrough curves from tracer tests usually are interpreted in terms of retardation coefficients, R. The retardation coefficient is often defined as:

$$R = 1 + \frac{1-p}{p}\rho_s K_d \qquad (6\text{-}8)$$

where K_d is the sorption distribution coefficient (m^3/kg) and ρ_s is the density of the solid (kg/m^3). In a cross-hole test with a uniform velocity, the retardation coefficient indicates how much a sorbing tracer is retarded compared with a non-retarded tracer. For example, a tracer with R = 2 would have twice the residence time compared to a conservative tracer. In a SWIW test, this difference in travel time is much less apparent in the tracer recovery breakthrough curve compared with a cross-hole test. A sorbing tracer will travel outwards during the fluid injection phases with lower velocity than a conservative tracer, but will also travel equally slowly back to the borehole during the pumping phase. In the absence of dispersion, it is not possible in a SWIW test to distinguish two tracers with different retardation factors. However, in the presence of dispersion, a difference in retardation factor will indeed also result in a different recovery breakthrough curve.

Figure 6-19 illustrates the effect of a few different retardation factors on the recovery breakthrough curve, from a simulated SWIW tests without an ambient hydraulic gradient. Other parameters are as follows:

$T = 10^{-6}$ m^2/s.

p = 0.001.

Q = 350 ml/min.

Longitudinal dispersivity = 0.5 m.

Figure 6-19 shows that all four breakthrough curves look similar, but with relatively clear differences due to hydrodynamic dispersion. The curves differ at the peak and at the tail of the breakthrough curves. The effect would be expected to be more visible as dispersion is increased. Thus, it is conceivable that retardation factors may be estimated from a SWIW test, although much less clearly than compared with a cross-hole tracer experiment.

Estimation of retardation coefficients always, in any kind of tracer experiment, requires two or more tracers, preferably injected in the same injection solution. One tracer is conservative (or at least retarded less) and then one measures how much the other tracer is retarded compared to the other. In cross-hole tracer tests, this is a fairly common experiment. A sensitivity analysis was here carried out for the case recovery break-through data of two tracers with different retardation factors, injected simultaneously in a SWIW test, being evaluated simultaneously to determine parameter values. From the previously demonstrated difficulty to simultaneously estimate porosity and dispersivity values from a SWIW test, one might anticipate that estimation regarding sorbing tracers would be difficult as well.

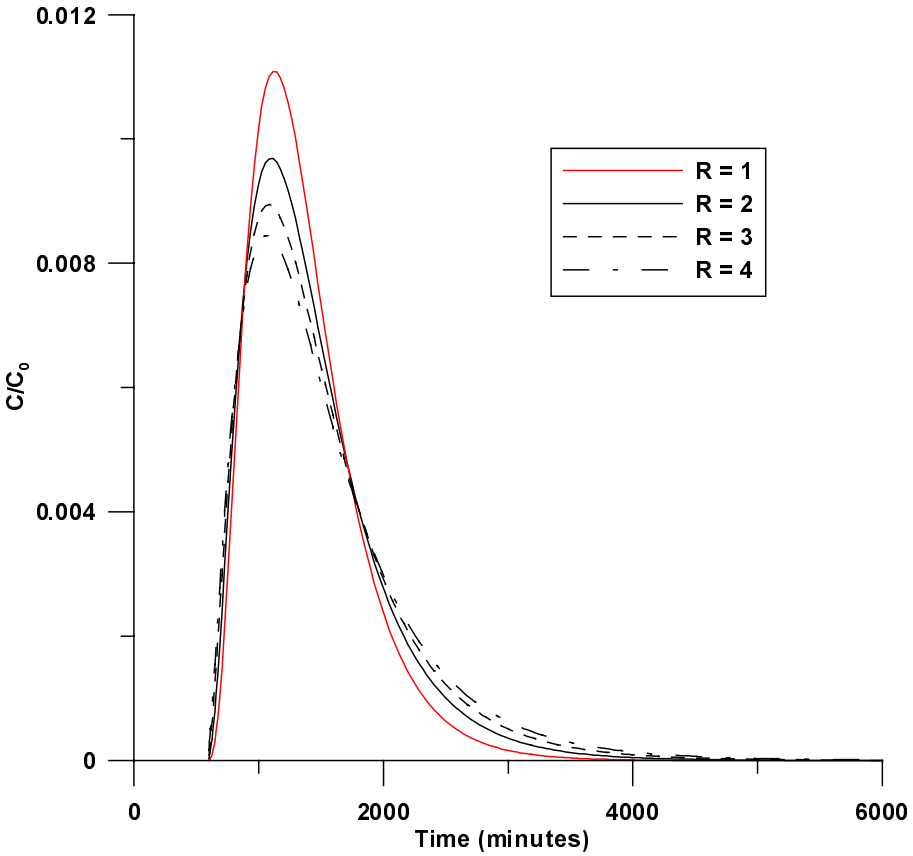

Figure 6-19. *Comparison of recovery breakthrough curves for tracer with different retardation factors.*

A simulation scenario with porosity, longitudinal dispersivity and the retardation factor as estimation parameters resulted, by calculating the parameter co-variance matrix, in very high (very close to 1 or –1) correlation values. Thus, these three parameters may not be estimated simultaneously from two tracer breakthrough curves obtained in a SWIW test. Further sensitivity analysis showed that if porosity is considered known, the dispersivity and the retardation factor may be estimated simultaneously. Similarly, if the dispersivity is considered known, the porosity and the retardation factor may be estimated simultaneously. It might be possible that the longitudinal dispersivity can be set to a fixed value, or that several values can be tried, and that estimated porosity values and retardation coefficients may be estimated with a certain degree of confidence. However, such and other possible estimation strategies are best tested with actual field data and not further investigated here.

Although not carried out here, it would be expected that the presence of a hydraulic gradient would create more favourable conditions for simultaneous estimation of porosity, dispersivity and retardation factors, analogous to the studied case in section 6.2.4.

Matrix diffusion

As an example of the behaviour of a time-dependent process during a SWIW test, a tracer undergoing diffusion into a stagnant solid matrix is simulated. In this example, the simulation is performed in a vertical section with radial symmetry instead of the previous areal simulation set-up. The simulated geometry approximately corresponds to a dual-porosity approach based on the assumption of parallel fractures and is schematically illustrated in Figure 6-20.

The solute transport is simulated with the standard advection-dispersion model in two dimensions. The dispersion coefficients in the longitudinal (D_L) and transverse (D_T) directions, respectively, are commonly expressed by:

$$D_L = a_L v + D_m \quad (6\text{-}9)$$

$$D_T = a_T v + D_m \quad (6\text{-}10)$$

where a_L and a_T are the longitudinal and transverse dispersivities, respectively, v is the magnitude of the water velocity and D_m is the diffusion coefficient. In the radial cross-section above, significant flow only takes place in the x-direction in the thin layer that represents the fracture and here the advective terms (a_L and a_T dominates). In the stagnant matrix the diffusion term dominates so that $D_L = D_T = D_m$.

The layout in Figure 6-20 represents a single plane-parallel fracture with a width of 0.001 m (half width = 0.0005 m) and a porosity of 1.0. The hydraulic conductivity, K, of the fracture is set to 10^{-3} m/s, which corresponds to a transmissivity of 10^{-6} m^2/s. The stagnant matrix (simulated with an extremely low value of hydraulic conductivity) extends, on both sides of the fracture, to a distance of 0.2 m away from the centre of the fracture. The model extends 50 m away in the radial direction, which is well beyond the distances that solute may travel during the fluid injection phases. A porosity value is assigned to the stagnant matrix as well as a diffusivity value. The latter is pore diffusivity, which is less than diffusivity in water due to tortuosity and constrictivity effects. The layout is also equivalent to a system having parallel fracture planes with a fracture spacing of 0.4 m, fracture widths of 0.001 m and a flow porosity of 0.0025.

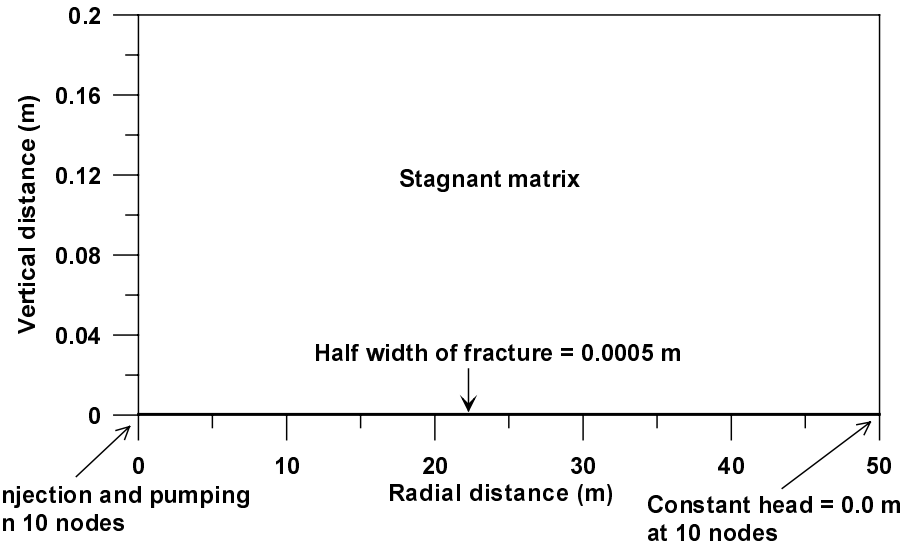

Figure 6-20. *Layout for simulation of SWIW test in a fracture with matrix diffusion.*

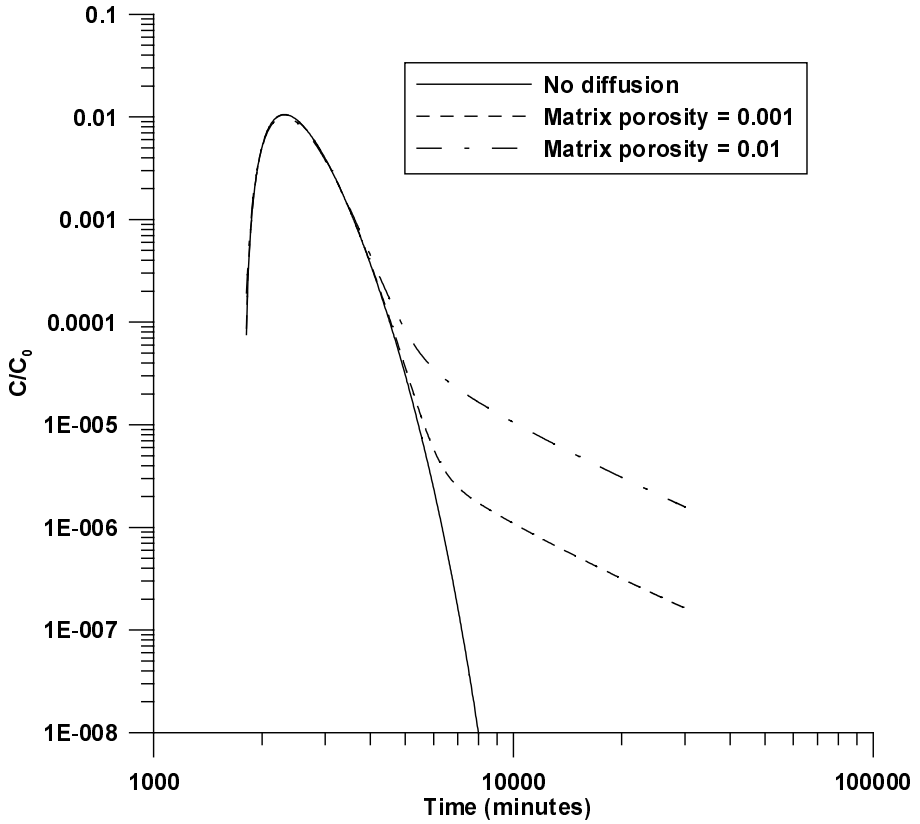

Figure 6-21. *Matrix diffusion effects on tracer recovery for two different matrix porosity values. Diffusivity is set to 10^{-10} m^2/s.*

The duration of the tracer injection and chaser fluid phases is the same as in the other examples, 10 minutes and 10 hours, respectively. The waiting phase duration is generally set to 30 hours after tracer injection start. Figure 6-21 shows simulated tracer recovery curves for two different cases with different matrix porosity values (0.001 and 0.01, respectively) and a relatively high diffusivity of 10^{-10} m^2/s.

Figure 6-21 (note the logarithmic scale) shows a typical tracer recovery breakthrough curve for a SWIW test with matrix diffusion affecting the tracer transport. Breakthrough is more or less identical in the ascending and peak parts of the curve. At some point in the tail the matrix diffusion effect causes a deviation from the case with no diffusion. The high matrix porosity case starts to deviate at around $C/C_0 = 2 \times 10^{-4}$ and at around $C/C_0 = 10^{-5}$ for the low porosity case. The slope of the curves affected by matrix diffusion approach the expected slope of –1.5 (if plotted in a log-log graph), which is the basic indicator for the presence of matrix diffusion in a SWIW test /Tsang, 1995b/.

The effect on tracer recovery if the waiting phase duration is increased is demonstrated in Figure 6-22, where the waiting phase duration is increased to 110 hours (110 hours since start of tracer injection).

In Figure 6-22, significant deviations from the curves with no diffusion occurs at approximate C/C_0-values of 1×10^{-6}, 2×10^{-6} and 4×10^{-6}, for waiting phase durations of 0, 20 and 110 hours, respectively. Thus, the effect of increasing the waiting time from 20 to 110 hours approximately doubles the concentration where diffusion starts to become visible. The concentration values are very low (relative to C_0) and will thus place high demands on the dynamic ranges of the tracers.

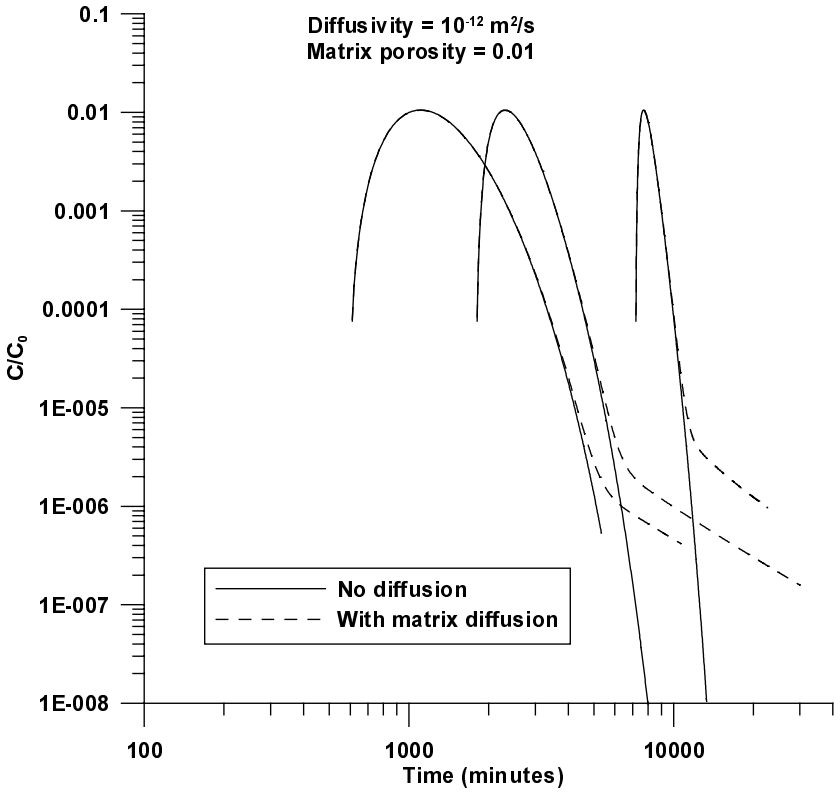

Figure 6-22. *Tracer recovery with different waiting phase duration. From left to right in the figure, the waiting phase duration is 0, 20 and 110 hours, respectively.*

Insufficient dynamic range of tracers may be alleviated to some extent by increasing the tracer injection duration. In Figure 6-23, the tracer injection duration is increased to 120 minutes instead of previously used 10 minutes. A tracer injection of 120 minutes may currently be regarded as an approximate upper limit for the injection duration when consideration has been taken to volumes of available storage vessels for tracer injection solution, the solubility of tracers, etc. The effect of increasing the tracer injection duration is fairly straightforward to describe. It increases the total injected tracer mass and thereby results in higher concentration levels in the recovery breakthrough curve. This effect also occurs for the concentration level when matrix diffusion effects become visible. The total effect is about one order of magnitude higher concentration levels, which, of course, reflects the magnitude of the increase in injected tracer mass.

Similar to previous examples, a sensitivity analysis shows that fracture porosity, dispersivity and matrix dispersivity may not be estimated simultaneously. Thus, although the characteristic late-time slope of the tracer recovery curve may identify the effect of matrix diffusion, estimation of its magnitude may require independent information on some other parameters.

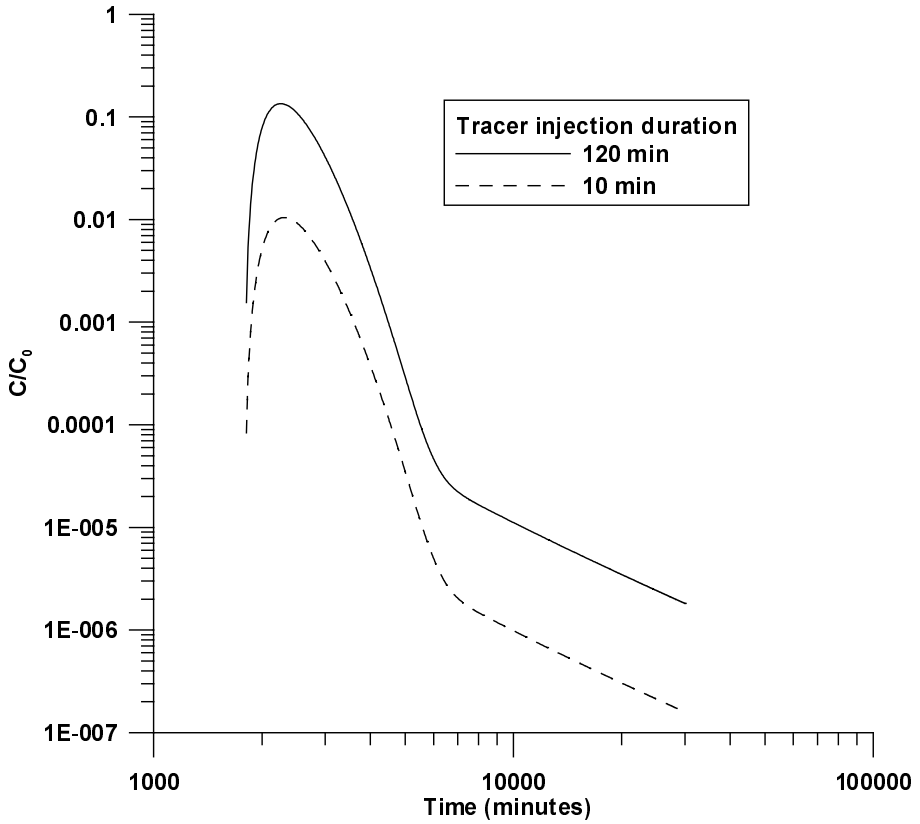

Figure 6-23. *Comparison of different tracer injection duration. The diffusivity is set to 10^{-12} m^2/s and the matrix porosity to 0.01.*

In summary of the scoping calculations concerning matrix diffusion, identification of this process may be possible if the effect is large (i.e. large matrix porosity and/or diffusivity). For smaller effects, the dynamic ranges of tracers become a limiting factor and experimental times may become large. Means to increase the possibility of identifying diffusion into a stagnant matrix, besides finding tracers with large dynamic ranges, include increasing the tracer injection duration and increasing the waiting phase duration.

The scoping calculations are made in very ideal systems and may not be considered as exact predictions of what may happen in an actual SWIW test. The only way to test if it is possible to identify a process such as matrix diffusion is to perform an actual field study in a borehole section with no or very low hydraulic gradient, maximise the injection concentration and injection duration and employ a relatively long waiting phase.

The diffusion process studied here is, of course, not the only possible time-dependent process. Other such processes may, for example, include other types of time-dependent surface sorption. In addition, the rates with which various processes occur may vary spatially.

6.3 Effects of heterogeneity on parameter identification

Ad advantage of SWIW tests is that, in principle, the identification of time-dependent processes, such as matrix diffusion, is not confused by spatial heterogeneity of medium properties. The reason for this is basically that the tracer experiences the same flow path, but in reverse directions, during both the fluid injection phase as well as the fluid extraction phase. However, as been mentioned earlier, studies have been made /Lessoff and Konikow, 1997; Altman et al., 2000/ that indicate that the presence of strong background hydraulic gradients may seriously disturb the reversibility of the flow field in heterogeneous features.

For the site investigation programme, relatively moderate gradients should be expected in the absence of shafts or tunnels. Thus, this should not present a significant problem for the site investigations. In addition, it was demonstrated earlier that also in homogeneous systems with a strong hydraulic gradient problems with tracer recovery might arise when long waiting times are used. Thus, it may be that only relatively short SWIW tests are performed in such environments and then matrix diffusion or other time-dependent processes may not be relevant to identify anyway. It should also be mentioned that the use of two or more different tracers with different diffusivity values, for example, should be expected to alleviate interpretation ambiguities as well.

For other parameters such as flow porosity and dispersivity, heterogeneity will present other interpretation considerations. For example, dispersion effects may be expected to be much less visible (i.e. smaller) in a SWIW test compared to a cross-hole tracer test because of the reversibility of flow paths. In cross-hole tracer tests, flow paths are not reversed and a larger spread in the arrival times of tracer should be expected (i.e. larger dispersivity).

Heterogeneity around a tested borehole section may cause the flow geometry to be different than the one used in this study (two-dimensional) and flow might be channelled into one or more dominating flow paths. Although the actual field geometry that the injected tracer experiences might differ from the ideal two-dimensional representation used here, the general findings from the scoping calculations should still be valid and field implementation should not be affected either by heterogeneity. A somewhat related problem is that independently estimated values of transmissivity (from injection tests, for example) and groundwater flow (from dilution tests) will be affected by the flow geometry around the borehole.

7 Results and recommendations

7.1 Experimental and hydraulic requirements

- The results from the literature review and scoping calculations in this report indicate that implementation of the SWIW method is feasible with the experimental and site requirements for the forthcoming SKB site investigation programme PLU. The dilution probe would likely be suitable for performing SWIW tests in expected conditions for the site investigation programme PLU.

- If in-situ tracer tests are to be performed within the site investigation programme to estimate/identify transport parameters/processes, SWIW tests are useful simply because it is the only available single-hole tracer test method for this purpose.

- Detailed design of each measurement should be made based on estimates of transmissivity and hydraulic gradient (or groundwater flux) from prior hydraulic testing and dilution measurements. This should be accomplished relatively easily by following some type of standardised protocol/procedure developed specifically for this purpose. Experimental strategy and goals are likely to depend on the hydraulic conditions in the test section.

- Design variables include:
  - Flow rates
  - Tracer injection duration
  - Chaser fluid duration
  - Waiting phase duration
  - Tracer injection concentration
  - Total experimental time

- Experimental design depends on:
  - Transmissivity
  - Hydraulic gradient

- A main difficulty from an experimental design perspective is to obtain a prior estimate of the advective porosity (or any other representation of the volume available for injected flowing water). This determines how far out into the formation the SWIW test reaches and also the plume drift in the case of an ambient hydraulic gradient. To somewhat alleviate this problem, a possible general strategy may be to maximise the injection and chaser flow rates given the experimental constraints regarding acceptable injection pressures (about 50 m head). Reasonable flow rates should range between about 25 ml/min to 300 ml/min.

- The choice of fluid injection method (i.e. by either constant flow or constant pressure) is likely not important from an interpretation point of view. Injection by constant flow is more practically feasible and should therefore be used.

- There appears to be no particular advantages of establishing steady state hydraulic conditions prior to tracer injection. Although storage effects may affect the temporal

distribution of hydraulic heads, there appears to be no significant effect on tracer recovery for reasonable values of storativity. This should also imply that it is acceptable that the injection flow is not constant, as there will be a certain build-up time in the beginning of the fluid injection.

- Experimental times will likely be different depending on porosity values, applied flow rates, etc. In cases of high porosity values (i.e. large fracture volume) it may be necessary to increase the chaser injection duration in order to obtain a more complete (i.e. the ascending part) recovery breakthrough curve. One should expect experimental time frames from a few days up to about 10–5 days.

- Increasing the duration of the chaser fluid injection causes longer experimental times and puts higher demands on dynamic ranges of tracers, but this may be necessary in low transmissivity formations.

7.2 Process identification and parameter estimation

- Porosity and longitudinal dispersivity may not be estimated simultaneously from the tracer recovery breakthrough curve. In order to estimate one of the parameters, the other must be known from independent measurements/estimates. This is a principal limitation compared to cross-hole tracer tests. However, in the presence of a hydraulic gradient these parameters may be estimated simultaneously, assuming that the hydraulic gradient may be estimated from independently determined transmissivities and flow rates. The gradient itself may not be estimated, if flow porosity and dispersivity also have to estimated simultaneously.

- The presence of an ambient hydraulic gradient may be an experimental design concern, i.e. excessive plume drift, for plausible extreme values of gradient, transmissivity and porosity. For expected natural conditions in Swedish bedrock, this will likely seldom be a significant problem. Close to shafts and tunnels, on the other hand, plume drift will likely have a relatively large impact on the choice of duration of the various experimental phases and flow rates. If the gradient is expected to be a problem, this may be alleviated by careful choice of flow rates.

- Retardation coefficients (linear sorption) are in principle possible to identify if two or more tracers are injected simultaneously. Analogous to the case of simultaneous estimation of porosity and dispersivity, estimation of retardation coefficients is less straightforward than for cross-hole tracer experiments.

- Matrix diffusion effects may be identified if diffusion rates and matrix porosity are sufficiently large. A requirement for this is to monitor the tail of the tracer recovery curve as long as possible. If the effect is low, the dynamic range of tracers is expected to be a seriously limiting factor. Means to alleviate problems with dynamic range of tracers are to increase the tracer injection duration (maximum is about two hours), injection concentration and also the waiting phase duration.

- Heterogeneity in the tested feature should not present any particular experimental or interpretation issues than compared with cross-hole tracer tests. On the contrary, SWIW tests are generally considered an approach to decrease confusion between

heterogeneity and time-dependent processes (i.e. matrix diffusion). However, strong hydraulic background gradient will offset this advantage and one should probably avoid to perform SWIW with long duration in such environments.

8 References

Altman S J, Jones T L, Meigs L C, 2000. Controls on mass recovery for single-well injection-withdrawal tracer tests. Chapter 4 in Sandia report SAND97-3109 (Meigs et al., editors).

Andersson P, 1995. Compilation of tracer test in fractured rock. SKB PR 25-95-05, Swedish Nuclear Fuel and Waste Management Co.

Bachmat Y, Mandel S, Bugayevski M, 1988. A single-well tracer technique for evaluating aquifer parameters, I. Theoretical work. Journal of Hydrology 99: 143–163.

Bear J, 1979. Hydraulics of groundwater. McGraw-Hill Inc., Israel.

Borowczyk M, Mairhofer J, Zuber A, 1967. Single well pulse technique in "Isotopes in Hydrology" (proceedings of Symp., Vienna). IAEA, Vienna, 507p.

Deans H A, 1971. Method of determining fluid saturation in reservoirs. U.S: Patent #3,623,842.

Drever J I, McKee C R, 1980. The push-pull test. A method of evaluating formation adsorption parameters for predicting the environmental effects on in-situ coal gasification and uranium recovery. In Situ 4: 181–206.

Fried J J, 1975. Groundwater pollution. Developments in Water Science, Vol. 4, Elsevier, Amsterdam.

Gelhar L W, Collins M A, 1971. General analysis of longitudinal dispersion in nonuniform flow. Water Resources Research 7: 1511–1521.

Gelhar L W, Welty C, Rehfeldt K R, 1992. A critical review of data on field-scale dispersion in aquifers. Water Resources Research 28, no. 7: 1955–1974.

Gustafsson E, 2001. Methods and instrumentation for groundwater flow measurements (in Swedish: "Metoder och utrustning för grundvattenflödesmätning"). SKB TD 01-53, Swedish Nuclear Fuel and Waste Management Co.

Güven O, Falta R W, Molz F J, Melville J G, 1985. Analysis and interpretation of single-well tracer tests in stratified aquifers. Water Resources Research 21, no. 5: 676–684.

Haggerty R, Schroth M H, Istok J D, 1998. Simplified method of "push-pull" test data analysis for determining in situ reaction rate coefficients. Ground Water 36, no. 2: 314–324.

Haggerty R, Fleming S W, Meigs L C, McKenna S A, 2000a. Evaluation of single-well injection-withdrawal tracer-test data with multirate-diffusion model. Chapter 6 in Sandia report SAND97-3109 (Meigs et al., editors).

Haggerty R, McKenna S A, Meigs L C, 2000b. On the late time behavior of tracer test breakthrough curves. Water Resources Research 36, no. 12: 3467–3479.

Haggerty R, Fleming S W, Meigs L C, McKenna S A, 2001. Tracer tests in fractured dolomite. 2. Analysis of mass-transfer in single-well injection-withdrawal tests. Water Resources Research 37, no. 5: 1129–1142.

Hall S H, Luttrell S P, Cronin W E, 1991. A method for estimating effective porosity and groundwater velocity. Ground Water 29: 171–174.

Istok J D, Humphrey M D, Schroth M H, Hyman M R, O'Reilly K T, 1997. Single-well "push-pull" test for in situ determination of microbial activities. Ground Water 35, no. 4: 619–631.

Istok J D, Field J A, Schroth M H, 2001. In situ determination of subsurface microbial enzyme kinetics. Ground Water 39, no. 3: 348–355.

Leap D I, Kaplan P G, 1988. A single-well tracing method for estimating regional advective velocity in a confined aquifer: Theory and preliminary laboratory verification. Water Resources Research 24, no. 7: 993–998.

Lee T-C, 1999. Applied mathematics in hydrogeology. CRC press LLC.

Lessoff S C, Konikow L K, 1997. Ambiguity in measuring matrix diffusion with single-well injection/recovery tracer tests. Ground Water 35, no. 1: 166–176.

McNeish J A, Andrews R W, Vomoris S, 1990. Interpretation of the tracer testing conducted in the Lueggern borehole. Nagra Technical Report 89-27.

Meigs L C, Beauheim R L, Jones T L, 2000. Interpretations of tracer tests performed in the Culebra Dolomite at Waste Isolation Plant Site. Sandia Report SAND97-3109. Available from U.S. Department of Commerce, National Technical Information Service.

Meigs L C, Beauheim R L, 2001. Tracer tests in fractured dolomite. 1. Experimental design and observed tracer recoveries. Water Resources Research 37, no. 5: 1113–1128.

Mercado A, 1966. Underground water storage study: Recharge and mixing tests at Yavne 20 well filed. Technical Report No. 12, TAHAL – Water Planning for Israel Ltd, tel Aviv.

Molz F J, Melville J G, Güven O, Crocker R D, Matteson K T, 1985. Design and performance of single-well tracer tests at the Mobile Site. Water Resources Research 21, no. 10: 1497–1502.

Nordqvist R, 2001. Effective sampling design for groundwater transport models. Ph.D. thesis, Uppsala University, Sweden.

Noy D J, Holmes D C, 1986. A single hole tracer test to determine longitudinal dispersion. Fluid Processes Research Group, British Geological Survey, Report FLPU 86-5.

Pickens J F, Grisak G E, 1981. Scale-dependent dispersion in a stratified granular aquifer. Water Resources Research 17, no. 4: 1191–1211.

Schroth M H, Istok J D, Haggerty R, 2001. In situ evaluation of solute retardation using single-well push-pull tests. Advances in Water Resources 24: 105–117.

Snodgrass M F, Kitandis P K, 1998. A method to infer in situ reaction rates from push-pull experiments. Ground Water 36, no. 4: 645–650.

Sutton D J, Kabala Z J, Schaad D E, Ruud N C, 2000. The dipole-flow test with a tracer: a new single-borehole tracer test for aquifer characterization. Journal of Contaminant Hydrology 44: 71–101.

Tomich J F, Dalton R L, Deans H A, Shallenberger 1973. Single-well tracer method to measure residual oil saturation. Journal of Petroleum Technology 25, no. 2: 211–218.

Tsang Y W, 1995a. Study of alternative tracer tests in characterizing transport in fractured rocks. Geophysical Research Letters 22, no. 11: 1421–1424.

Tsang Y W, 1995b. Discriminating effects of heterogeneity and matrix diffusion by alternative tracer designs. Lawrence Berkeley Laboratory report LBL-36831, University of California. Available from U.S. Department of Commerce, National Technical Information Service.

Voss C I, 1984. SUTRA – Saturated-Unsaturated Transport. A finite element simulation model for saturated-unsaturated fluid-density-dependent ground-water flow with energy transport or chemically-reactive single-species solute transport. U.S. Geological Survey Water-Resources Investigations Report 84-4369.